Evaluating Particle Migration Through A Geotextile Filter Cake Using Fluorescent Microspheres

by

Narges Karamizadeh

Submitted in partial fulfilment of the requirements
for the degree of Master of Applied Science

at

Dalhousie University
Halifax, Nova Scotia
March 2023

Dalhousie University is located in Mi'kma'ki, the
ancestral and unceded territory of the Mi'kmaq.
We are all Treaty people.

© Copyright by Narges Karamizadeh, 2023

DEDICATION PAGE

To my beloved parents whom without their support, encouragement, and sacrifice none of my achievements would be possible.

TABLE OF CONTENTS

LIST OF TABLES

LIST OF FIGURES

ABSTRACT

Viable dewatering techniques are an effective method to manage large volumes of contaminated, high-water content dredged sediments but the passing of small particles with attached organic contaminants during dewatering can create challenges for environmental remediation, if not properly contained. Better understanding of the mechanisms of this particle transport through laboratory experiments are necessary.

In this research, fluorescent microspheres (i.e., flurospheres ©) are proposed to be used to simulate small particles during the dewatering process. Methods to visualize and quantify these microspheres for dewatering research are developed and validated. Application trials of these experimental methods are then performed to examine the behaviour of small particles during dewatering of two different sediments. It is shown that the methods developed in this thesis can be used in these experiments to help better understand the attachment and detachment of particles during geotextile dewatering.

LIST OF ABBREVIATIONS USED

#/µl	Number per microliter
µl	Microliter
µm	Micrometer
AD	Anderson-Darling
AOS	Apparent Opening Size
CoA	Certificate of Analysis
GD	Geotextile dewatering
g	gram
GT-500	Geotextile #500
ICP-OES	Inductively Coupled Plasma Optical Emission Spectrometry
MC	Moisture Content
mg	Milligram
mg/l	Milligram per liter
Min	Minute
mL	Millilitre
MS	Microsphere
nm	Nanometer

SEM	Scanning electron microscope
TSS	Total suspended solids
ul	Microliter

ACKNOWLEDGEMENTS

I want to express my deepest appreciation to my advisor Dr. Craig Lake, for being a great mentor for me. It was a privilege to be supervised by a world class researcher and a true expert like him. Without his guidance, encouragement and support this dissertation would have not been possible. Many thanks to my committee members, Dr. Rob Jamieson and Dr. Gordon Price for their time, dedication, and interest.

I am grateful to Yan Nan Huang not only for all her help in carrying out my experiments but also for being kind, caring and supportive throughout my PhD program. I would also like to extend my gratitude to the Civil Department and CWRS. To the lab technicians: Heather Daurie and Dean Grijm, thank you for all your assistance along the way.

I owe much gratitude to my hard-working parents Askar Karamizadeh and Manzar Karamizadeh for all the sacrifices they have made, their love and endless care.

Thanks!

1 Introduction

1.1 General

The storage and disposal of contaminated, high-water content dredged sediments can be both an environmental and economic concern (Berilgen & Bulut, 2016). Viable dewatering techniques play a crucial role in managing large volumes of contaminated, high-water content dredged sediments so that the total volume of these sediments can be reduced for practical and economical disposal considerations (Lawson, 2008; Yee et al., 2012; Yee & Lawson, 2012). Geotextile dewatering is a practical approach for separating the solids and liquid portions in high water-content sediment using geotextile fabric as the filter media (Kutay & Aydilek, 2004; Bhatia & Liao, 2005). In this process, a sediment slurry is pumped into a geotextile tube, where the geotextile acts as a filter as the liquid is expelled through the pores of the geotextile, while most of the sediment solids are retained within the geotextile tube. Geotextile tubes are repeatedly filled until an insignificant amount of filtrate passes through the geotextile (Lawson, 2008).

Geotextile dewatering results in a layer of solids (filter cake) being deposited on the surface of the geotextile, which promotes retention and dominates subsequent filtration behaviour. Filtration is primarily controlled by the filter cake properties, rather than the geotextile properties. The filter cake formation and stability depend on the particle size distribution of the solids in the sediments, the concentration of particles, the flow rate, the applied pressure on the geotextile, as well as the structure of the geotextile (Alimohammadi & Lake, 2022). Many researchers have evaluated geotextile dewatering characteristics such as dewatering efficiency (i.e. how much the solids content can be increased) and dewatering rate (i.e. how long it will take) using small and large-scale laboratory tests (Moo-Young &

Ochola, 1999; Moo-Young et al., 2002; Mori et al., 2002; Huang & Koerner, 2005; Koerner & Koerner, 2006; Liao & Bhatia, 2005; Liao & Bhatia, 2006; Muthukumaran & Ilamparuthi, 2006; Liao, 2008; Huang & Luo, 2007; Satyamurthy, 2008; Segre, 2013; Bhatia et al., 2013; Weggel & Ward, 2012).

Successful dewatering of contaminated sediment via geotextile tubes requires that contaminants associated with the sediment do not migrate uncontrolled during the dewatering process. The general topic of particle transport through porous media has been the subject of many studies in the literature related to particles such as viruses, colloids, bacteria, and clay minerals (Sen & Khilar, 2006; Molnar et al., 2015; Petosa et al., 2010; Grasso et al., 2002; Bradford & Torkzaban, 2008; Vecchia et al., 2009; Sun et al., 2015; Dong et al., 2017; Feriancikova & Xu, 2012; Chowdhury et al., 2015; Fan et al., 2015; Tong et al., 2005; Godinez & Darnault, 2011; Tian et al., 2010; Lin et al., 2012; Thio et al., 2012; Guzman et al., 2006; Lahlou et al., 2000; Williamson et al., 2006; Jin & Flury, 2002; Chattopadhyay & Puls, 2000; Sobsey & Meschke, 2003). Understanding the various factors that control the migration of sediment particles during dewatering can assist in better understanding of risk of contaminant migration during this dewatering process.

The size distribution of suspended particulate matter in a liquid is of great importance in determining the transport and fate of these particles and associated contaminants during dewatering. Processes such as aggregation and adsorption depend on particle size (Zhang et al., 2018). Figure 1-1 shows typical size ranges for various particles that usually exist in natural systems (Stumm, 1977). The suspended particles most relevant in the dewatering of contaminated sediment are in the clay and colloidal size ranges (micrometre and sub-micrometre). Colloids can be defined in many different ways, depending on the application,

but in this thesis, colloids and suspended particles will be referred to as simply “particles”. In this thesis, these various size ranges will simply be referred to as “particles”.

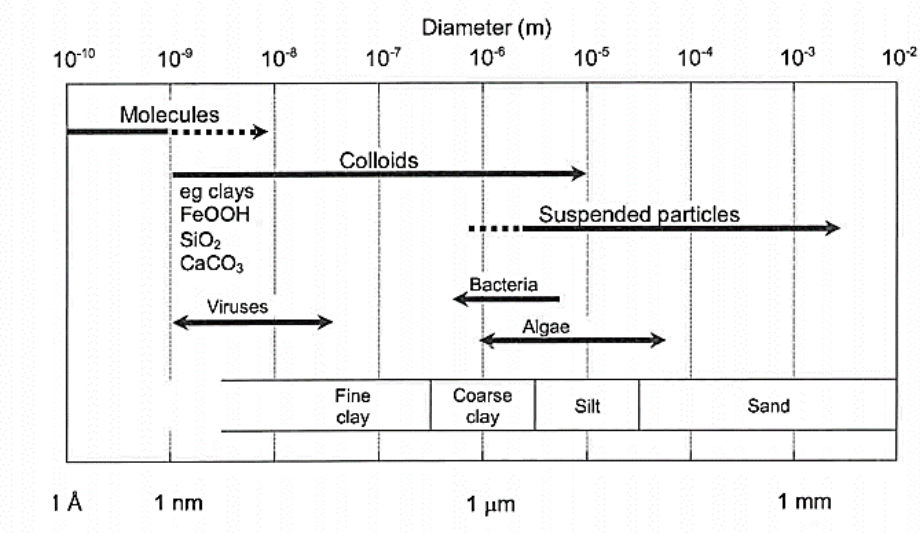

Figure 1-1 Common particle size definitions (taken from Stumm, 1977)

Figure 1-2 illustrates three mechanisms that can limit particle migration through porous media. If particles are comparable to, or larger than, the pore size of porous media, penetration will not occur and the filter cake will form above the media instead (McDowell-Boyer et al., 1986). In this case, substantial particle accumulation can decrease the filter system's permeability as fluid flows through the filter. It is also possible to mechanically remove particles during the filtration process by smaller pores being strained within the porous media. The number of particles that can accumulate during particle straining is limited, so there is only a slight decrease in permeability (McDowell-Boyer et al., 1986). Surface interactions between particles and the porous media can be a source of physical and chemical attraction that can also remove small particles from the solution (McDowell-Boyer et al., 1986).

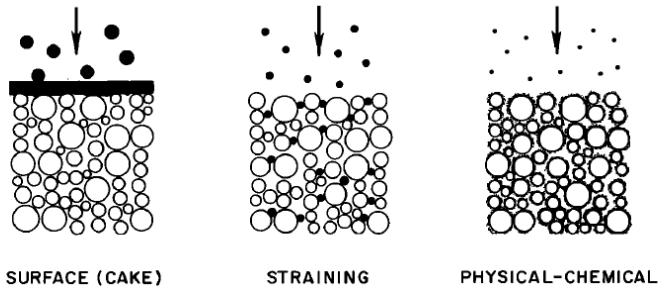

Figure 1-2 Illustration of three different types of filtration mechanisms (taken from McDowell-Boyer et al., 1986)

Specific physicochemical factors affecting particle transport and retention in porous media previously investigated include ionic strength, organic matter content, temperature, flow rate, surfactants, pH, and input concentration (e.g., Sun et al., 2015; Dong et al., 2017; Feriancikova & Xu, 2012; Chowdhury et al., 2015; Liu et al., 2015; Fan et al., 2015; Qi et al., 2014; Wang et al., 2017; Tong et al., 2005; Godinez & Darnault, 2011; Wang et al., 2012). Espinasse et al. (2007), Lin et al. (2012), and Thio et al. (2012) have showed that the presence of organic matter enhances the mobility of nanoparticles. Guzman et al. (2006) illustrated that as the pH approaches the point of zero charges of nanoparticles, the size of nanoparticle aggregates increases and nanoparticles' mobility decreases.

Research conducted to study the influencing factors in colloid transport (Grolimund et al., 1998; Ryan & Elimelech, 1996) in soils and aquifer environments has shown that when the chemistry of a solution changes, mobile colloidal particles can form. The rates of colloid release, caused by an abrupt increase in solution pH, increased as ionic strength decreased; due to changes in surface charge of the colloids (Ryan & Gschwend, 1994). The transport of viruses has been shown to be affected by several factors, such as solution chemistry, virus properties, soil properties, temperature, association with solid particles, and water

content (Jin & Flury, 2002). A few factors affecting bacteria transport in soils are grain size (Sharma & McInerney, 1994), cell surface properties (Gannon et al., 1991), physical heterogeneity (Harvey et al., 1993), pH and ionic strength (Jewett et al., 1995). Many studies have modelled the reduction in colloid retardation (Corapcioglu & Jiang, 1993; Flury & Qiu, 2008), colloid-associated contaminant transport (Ouyang et al., 1996; Ryan & Elimelech, 1996; de Jonge et al., 2004; Sen & Khilar, 2006), colloid transport in saturated porous media (Molnar et al., 2015), colloid transport in unsaturated porous media (DeNovio et al., 2004), and interaction forces (Petosa et al., 2010; Bradford & Torkzaban, 2008).

The work presented in this thesis attempts to use existing knowledge of colloid/virus/bacteria transport through porous media to further examine particle transport through filter cakes developed on geotextiles during geotextile dewatering. This thesis will focus on developing test methodologies using fluorescent microspheres as a physical model for small particles as filtration occurs in a geotextile dewatering situation. The following sections will provide the reader with some background information related to: 1) microspheres, and, 2) particle transport through geotextiles during dewatering.

1.2 Microspheres

Microspheres (MS) are manufactured particles that can simulate small particulates in the laboratory for geotextile dewatering tests. Employing microspheres in controlled experiments can effectively investigate the migration of particles and associated contaminants in porous media. Included in this section are research studies conducted by others to examine the fate and transport of various microspheres in different applications.

MS are spherical particles and describe a general class of particulates with diameters in the high nanometer to micron range (Shirvan et al., 2021). MS can be manufactured from various natural and synthetic materials (usually biodegradable and biocompatible polymers) and can serve as a reasonable surrogate for particle transport (Cospheric LLC, 2020). The microspheres' physicochemical properties that can be specifically tailored to the desired application are specific density, surface charge, and hydrophobicity (Klauth et al., 2007). MS have also demonstrated many advantages as a field tracer (Becker et al., 2004). They have known surface characteristics based on the materials used in manufacturing and can be readily counted by fluorescent microscopy. They have the advantage of not undergoing degradation in the subsurface and application rates can be easily controlled (Cospheric LLC, 2020; Cey et al., 2009).

Many researchers have carried out experiments and investigated microsphere's mobility in different porous media at different scales (Bradford et al., 2012; Camesano et al., 1999; Zvikelsky et al., 2008; Zvikelsky & Weisbrod, 2006; Ochiai et al., 2010; Close et al., 2006). Klauth et al. (2007) used microspheres as model colloids for transport experiments. Mishurov et al. (2008) measured carboxylate-modified microsphere (polystyrene latex microspheres) concentrations by fluorescence spectrophotometer and examined various factors, including flow rates, microsphere size, pH, and ionic strength. Magal et al. (2011) studied the migration of fluorescent carboxylate-modified latex (CML) microspheres through saturated sand columns of different sizes in laboratory experiments and simulated with mathematical models. The concentration was analyzed using fluorescence spectrophotometry. Colloid transport was found to be related to the solution salinity. Porubcan and Xu (2011) investigated the transport of carboxylated latex microspheres

(Magsphere Inc.) in heterogeneous porous media (quartz sands) through column transport experiments. Images of the latex particles were obtained using a scanning electron microscope. It was found that finer sand fractions result in more significant straining of colloidal particles within heterogeneous sand mixtures.

Klauth et al. (2007) analyzed MS concentrations in samples using two different methods: (i) direct surface counts (fluorescence microscope-surface counts of MS were carried out by photographing at several focus levels and manually overlaying the images for total counts) and (ii) counts from suspended samples with microscope.

1.3 Mobility of Particles/Contaminants During Geotextile Dewatering

Geotextile dewatering of sediments makes it possible to retain almost 100% of fine-grained material, and consequently, many contaminants associated with sediment can be retained (Fowler et al., 1996). Geotextile dewatering effectiveness can be maximized by developing what is known as a filter cake adjacent to the geotextile (Mastin et al., 2008). After filter cake creation, water associated with the material is allowed to drain through the filter cake. When a filter cake accumulates on the surface of a geotextile, the quality of the filtrate regarding particle contaminants is improved as particle straining occurs. Additional treatment may be needed if the filtrate contains additional contaminants (Tackley et al., 2021).

Many researchers, such as Lawson (2008), Mastin et al. (2008), and Yee et al. (2012), have reported successful applications of geotextile tube dewatering of contaminated sediments, providing site-specific information. A study by Tackley et al. (2021) conducted bench and

field scale experiments. They examined the effect of a filter cake deposited on the geotextile on the mobility of three metals (Cu, Pb, Zn) during the filtration of contaminated sediment. As a filter cake buildup occurred, the filtrate quality improved with respect to metal and particulate contaminants suggesting that filter cake presence may significantly influence the efficiency of contaminants filtration through geotextile dewatering. Alimohammadi et al. (2020) examined how the filter cake and pressure affect particle matter concentration in the effluent after geotextile dewatering. In this same study, particle transport was simulated using HYDRUS to investigate possible mechanisms that might contribute to particle movement through the filter cake. Based on HYDRUS model outputs, both attachment and detachment mechanisms were suggested to be involved in the fate and transport of particles during geotextile dewatering. However, it was acknowledged that it was difficult to assess the actually mechanism with this type of testing. Alimohammadi et al. (2019b) evaluated dewatering potential and filtrate quality (TSS) using sediment taken from the BH stabilization lagoon pilot area, following treatment with an optimal polymer dosage and filtration through GT-500 textile. A bench-scale analysis was conducted to determine the potential effectiveness of the technique. After filtration, the authors report a reduction of 98.8% in TSS. A filter cake (with a solids content by mass of 7.4 %) was found to have accumulated on the geotextile surface after 195 mL of the filtrate was produced (from 200 mL input).

1.4 Research Objectives

To better understand fate and transport of particles, it is hypothesized that microspheres can be used to play the role of particulate matter transporting associated (i.e. attached) contaminants in porous media. The research in this thesis is intended to develop testing

methods using microspheres that involve geotextile dewatering tests to expand the available testing methods to assess a particle's transport during the geotextile dewatering process. There are few, if any, studies in the literature that have used microspheres to simulate particle transport during dewatering. This thesis attempts to address the following specific research questions:

- How can we measure microsphere fate and transport in the laboratory during geotextile dewatering?
- What can we use as an experimental test setup to assess the fate and transport of microspheres during the geotextile dewatering process?

1.5 Organization Of Chapters

This thesis contains five chapters. A summary of the content of each chapter is presented below:

Chapter one introduced the research subject and outlined the objectives of the study. In addition, it has provided background information and definitions on microspheres, as well as available literature on particle transport through the soil. Also reviewed was particle transport during geotextile dewatering.

Chapter two provides information on the materials and methods used in this thesis.

Chapter three presents development of the microsphere techniques.

Chapter four presents the results of the experimental program designed to study the microsphere transport through filter cake during the geotextile dewatering process.

Chapter five provides the summary and conclusions of the thesis. Recommendations for future work are also presented in this chapter.

2 Materials and Methods

2.1 Introduction

The focus of this chapter is to provide information on the materials and methods used to conduct this study. Several materials were used in this study, including two soils that were developed with specific grainsize distributions, a woven geotextile, and carboxylate-modified microspheres (i.e. Fluospheres ©). The geotextile dewatering apparatus is the primary experimental tool in this study. The other major equipment employed to conduct the study were an optical microscope with camera and spectrophotometer.

2.2 Geotextile

A GT-500 geotextile was used in all experiments reported in this thesis (TenCate Corporation, 2015). As shown in Table 2-1, this polypropylene woven geotextile has a reported apparent opening size (AOS) of 430 μm, and pore size distributions of O_{50} and O_{95} of 80 μm and 195 μm, respectively.

Table 2-1 GT – 500 Properties (TenCate Corporation, 2015; Tackley, 2019)

Mechanical Properties	Test Method	Unit	Minimum Average Roll Value	
			MD	CD
Wide Width tensile strength (at ultimate)	ASTM D4595	KN/m (lbs/in)	78.8 (450)	109.4 (625)
Wide width tensile elongation	ASTM D4595	%	20 (max.)	20 (max.)
Factory seam strength	ASTM D4884	KN/m (lbs/in)	70 (400)	
CBR Puncture strength	ASTM D6241	N (lbs)	8900 (2000)	
Apparent opening size (AOS)	ASTM D4751	Mm (U.S. SIEVE)	0.43 (40)	
Water flow rate	ASTM D4491	l/min/m^2 (gpm/ft^2)	813 (20)	
UV Resistance (% strength retained after 500 hrs)	ASTM D4355	%	80	
Filtration Properties	Test Method	Unit	Typical Value	
Pore size distribution (O50)	ASTM D6767	Micron	80	
Pore size distribution (O95) *	ASTM D6767	Micron	195	
Filtration Properties	Test Method	Unit	Typical Value	
Mass/Unit Area	ASTM D5261	g/m2 (oz/yd2)	585 (17.3)	
Thickness	ASTM D5199	mm (mils)	1.8 (70)	

2.3 Geotextile Dewatering (GD)

Figure 2-1 shows the geotextile dewatering test apparatus used in this thesis, consisting of a middle chamber, a geotextile specimen, a rubber o-ring, and a lower chamber. This apparatus is similar to that used by Alimohammadi and Lake (2022).

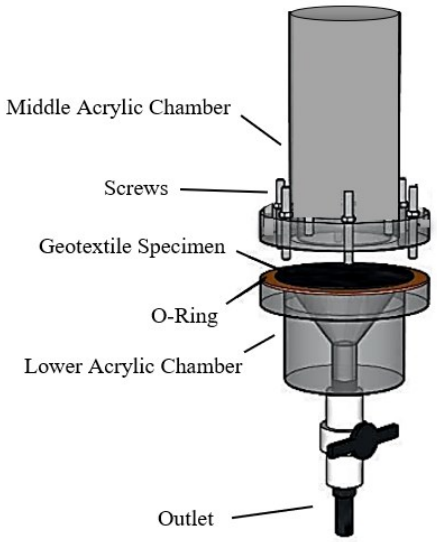

Figure 2-1 Geotextile dewatering test apparatus (Modified from Alimohammadi and Lake, 2022)

To examine microsphere migration, geotextile dewatering (GD) tests were performed. The GD test apparatus employed in this study (Figure 2-1) was a modified version of the apparatus that Alimohammadi and Lake (2022) used in their study. In this study, all tests were conducted under atmosphere pressure conditions (i.e. no pressure applied).

2.4 Soil Used in Dewatering Tests

Soil used for dewatering tests in this study was obtained from Dartmouth, Nova Scotia. The soil is a commonly found sandy silt/silty sand glacial till in the area. The sample was taken

with an excavator, at a depth well below the rootmat/organic layer. Hence it is anticipated to have minimal organic matter present. To prepare samples, soil was oven dried at 110ºC and then passed through sieve No. 4. Soil particle sizes were then separated on the following sieve sizes for future composition of samples for dewatering tests: No. 4, 8, 16, 30, 50, 100, 200 and passing 200.

Table 2-2 provides the two grain size distributions created from this soil for the testing program in this thesis. These grain size distributions were based on trying to develop a grain size that would allow reasonable test times during filtration, generate sufficient sediment in the filtrate, and allow some retention of the microspheres in the filter cake.

Table 2-2 Two grain size distributions developed for this thesis.

Sieve No.	Sieve Size (mm)	Soil 1 Percent Passing (%)	Soil 2 Percent Passing (%)
4	5	100	100
8	2.36	100	85
16	1.18	85	68
30	0.6	68	50
50	0.3	50	30
100	0.15	30	15
200	0.075	15	10

2.5 Carboxylate-Modified Microspheres

Fluospheres© are the trade name of the microspheres used in this study to perform filtration experiments (Figure 2-2). This fluorescent microsphere is loaded with proprietary dyes that allow them to be illuminated with ultraviolet (UV) light. Under UV illumination, these microspheres can emit intense colour, improving contrast and visibility relative to background material (Thermo Fisher Scientific, 2022). Fluorescence occurs when a

molecule absorbs light energy and immediately releases it as light again. Two different carboxylate fluospheres were used in this research. The first was yellow-green coloured sphere with a nominal diameter of 1.0 µm, solids percentage of 2%, and excitation/emission wavelength of 505/515 nm (Thermofisher catalogue number F8823). The certificate of analysis (CoA) on the fluosphere bottle indicated that the concentration of the fluosphere was 4.6 x 10^9 particles/mL. The second one was red with a nominal diameter of 2.0 µm, a solids percentage of 2%, an excitation/emission wavelength of 580/605 nm (ThermoFisher catalogue number F8826). The surface charge on the red microspheres was 0.0074 meq/g which is not high compared to organic matter found naturally in soils.

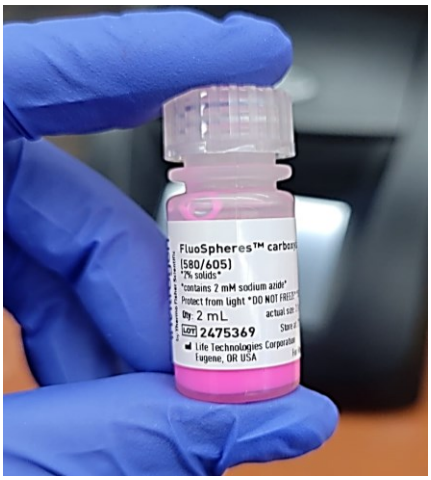

Figure 2-2 Red fluospheres used in this research.

Based on recommendations of the manufacturer, the fluospheres were refrigerated at 2–6°C and protected from UV light. Before sampling, the fluosphere bottle was mixed by sonication for 5 minutes (as recommended) using the bath sonicator in the Water Lab at Dalhousie University.

2.6 Microsphere Measurement Equipment

Below is a description of the equipment used to visualize and count microsphere concentrations used in the dewatering tests, as well as to determine total suspended solids (TSS) generated from the dewatering tests.

2.6.1 Microscope

Figure 2-3 shows the Eclipse 80i Upright Microscope with a D-FL epi-fluorescence attachment (Nikon Canada, Mississauga, ON) employed in this study to visualize and measure the Fluospheres in the samples (Nikon Instruments Inc., 2022).

The excitation/emission wavelengths of yellow-green and red fluospheres used in this study were 505/515 and 580/605 respectively and were identified with the microscope by using a filter inserted in the microscope. The microscope filter used in this study was a Nikon triple band DAPI-FITC-Texas Red Filter (Excitation: 395-410 nm, 490-505 nm, 560-580 nm; Emission: 450-470 nm, 515-545 nm, 600-650 nm). Images of the samples under the microscope were taken at 40, 100, and 400 magnification with a Nikon DS-Fil camera connected to NIS-Elements BR 2.30 image analysis software program (Nikon Instrument Inc., 2022).

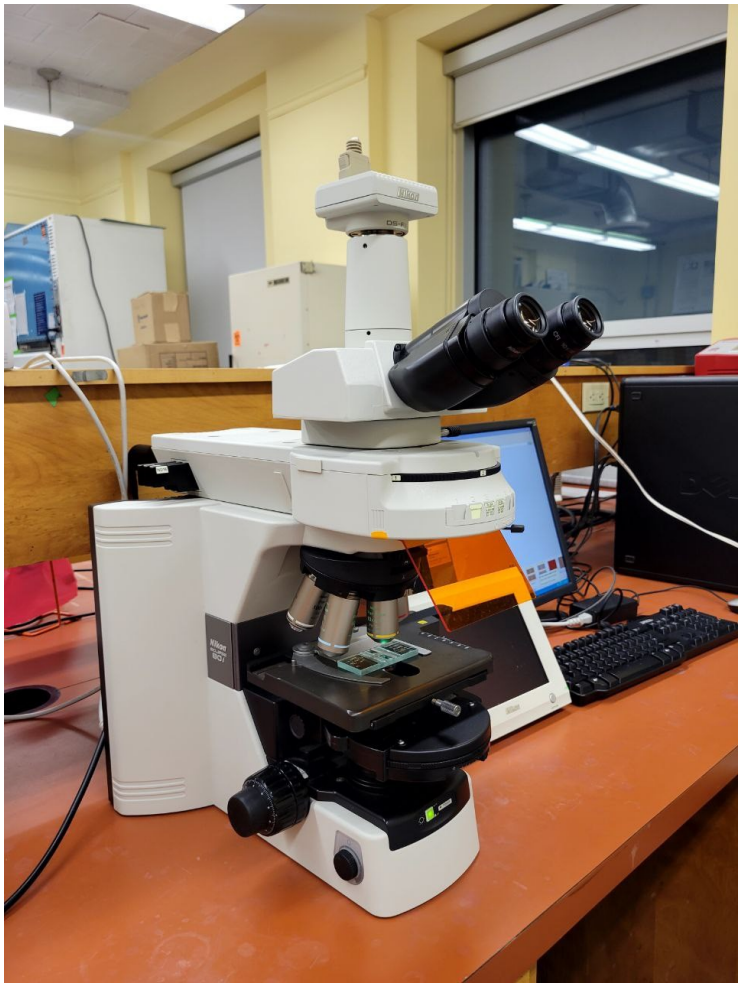

Figure 2-3 Eclipse 80i microscope used in this research.

Counting slides were used for manual counting of microspheres under the microscope with two gridded counting areas containing 16 large square areas each. With 16 small squares in each large square, each counting area has 256 small rectangles. Two gridded areas are separated by an H-shaped “moat”. The chamber is engraved with perpendicular lines etched using a laser (Figure 2-4). By looking at a defined area of the grid, it is therefore possible to count the number of microspheres for a specific volume of fluid. This enabled

the potential to calculate the concentration of particles in the fluid under investigation. The chamber is supplied with a thin glass cover (Hausser Scientific, 2022).

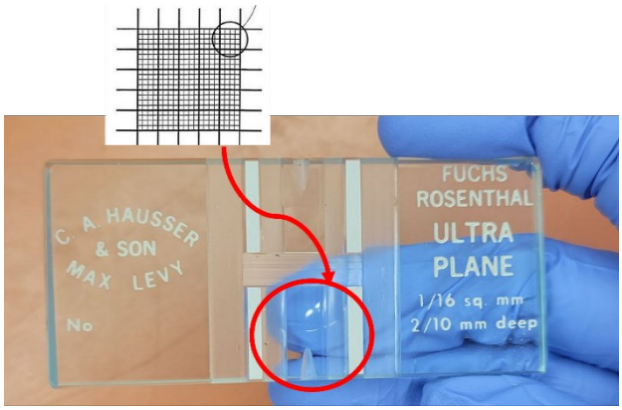

Figure 2-4 Counting slide used to determine microsphere concentrations in samples.

2.6.2 HACH DR 6000 Benchtop Spectrophotometer

The HACH DR 6000 benchtop spectrophotometer was used to measure the amount of total suspended solids (TSS) in samples. In this case, 10 mL of sample was placed in a glass sampling jar and inserted into the machine for each trial. The machine was calibrated before each test with a 10 mL sample of Milli-Q water. The effective measurement range of the unit was 5 to 750 mg/L TSS (HACH Company, 2014). Those samples which exceeded the upper limit were diluted with Milli-Q water and retested. These values were then multiplied by the appropriate dilution factor to obtain results.

2.7 Dewatering Test Procedures

Step 1 of the geotextile dewatering tests began with the given soil grain size distribution being made into a slurry. The amount of soil added to the 1 L of water was varied in order to generate different thicknesses of developed filter cakes during dewatering tests. Slurries were made to initial water contents of 1000%, 500%, and 333.33% (i.e. 100 g, 200 g, and

300 g of soil added to 1 L of water, respectively). These water contents were selected to simulate those typical slurries pumped into geotextile containers in field applications (Kutay & Aydilek, 2004). Slurries were then carefully poured into the GDP apparatus cylinder. During the slurry dewatering process through the geotextile, a layer of the filter cake was developed on the geotextile. Filtrate from the dewatering process was then collected in glass containers throughout the outlet, at each 250 ml of filtrate (totalling 1000 mL).

After this process was complete, Step 2 involved passing a solution of water and fluospheres at a concentration of 10^{-4} ml of fluospheres/ml of water through the filter cake and geotextile. The concentration of fluospheres in the collected filtrates was then measured using the microscope technique described previously. In addition, the collected filtrate samples were tested for TSS.

Step 3 of this process involved passing 1000 ml of distilled water through the developed filter cake after solution dewatering, to determine the number of microspheres detached from the filter cake. Filtrate was collected every 250 mL. TSS measurements were also performed on all filtrate samples.

These three steps were performed again (i.e. new tests) with the same soil (i.e. soil mixture 1), but at two larger filter cake thicknesses (i.e., slurries made of 200 g and 300 g soil). These three tests were repeated using a different soil grain size distribution (soil mixture 2). In total, there were six sets of tests, each of which included the steps of 1) filter cake development, 2) microsphere solution dewatering, and, 3) water filtration. In total, 18 steps were performed with four 250 ml filtrate samples collected from each step resulting in 72

filtrate samples being collected. Table 2-3 lists all the steps and measurements performed for each test and Table 2-4 lists the different tests performed in the thesis.

Table 2-3 Summary of the various steps performed within this thesis.

Test	Filtrate sample	Number of Microscope Measurements	Number of TSS Measurements on Filtrate Sample
Filter cake development	1	-	1
	2	-	1
	3	-	1
	4	-	1
Microsphere solution dewatering	1	10	1
	2	10	1
	3	10	1
	4	10	1
Only water filtration	1	10	1
	2	10	1
	3	10	1
	4	10	1

When samples were required for microsphere visualization and quantification, ten 2 µl samples were extracted from each of the 250-ml filtrate samples.

Table 2-4 Summary of Tests Performed in the Thesis.

Test	Filter cake development (Measurement of TSS)	Microsphere solution passed through filter cake (Measurement of TSS, microsphere)	Distilled water passed through filter cake (Measurement of TSS, microsphere)
100 g of Soil Mixture 1	Yes (duplicate)	Yes (duplicate)	Yes (duplicate)
100 g of Soil Mixture 2	Yes	Yes	Yes
200 g of Soil Mixture 1	Yes	Yes	Yes
200 g of Soil Mixture 2	Yes (duplicate)	Yes (duplicate)	Yes (duplicate)
300 g of Soil Mixture 1	Yes	Yes	Yes
300 g of Soil Mixture 2	Yes	Yes	Yes

This chapter has provided an account of the materials and methods employed in this study to investigate the fate and transport of microspheres through a geotextile filter cake. The following chapter will present the process used to validate some of the microsphere testing methods for the method development of this thesis.

3 Microsphere Concentration Method Development

Given that the type of testing presented in this thesis has not previously performed in the literature for geotextile filtration testing, it was necessary to develop and validate some of the test methods adopted in this study, with a particular focus to geotextile dewatering applications. This chapter describes the various testing performed to gain confidence in the method, as well as establish its accuracy and variability.

3.1 Development of Microsphere Visualization Methods

Initial attempts at microsphere visualization with the microscope involved preparing distilled water solutions with the 1um yellow-green microsphere. To prepare solutions for visualization, 0.1 mL of the microspheres were sampled by pipette and diluted into 1000 mL of DIW to form a microsphere concentration of 4.6×10^5 particles/ mL. This solution was then shaken to ensure homogenization of the sample. A subsample (2 µl) of this solution was then sampled with a pipette, placed onto a counting slide, and the slide placed under the microscope. The slide-grid area, consisting of 256 squares, was covered by the entire 2 µl of the sample. Two different magnifications were used to visualize the images (100x and 400x) for comparison purposes. Figure 3-1 shows an image captured from the microscope for the 100x magnification. The microspheres can be seen in the image but appear quite small and relatively faint. Figure 3-2 shows the improvement of visualization of the microspheres at 400x magnification. Although the 400x magnification improved the visualization, less than one counting square is visible at this magnification.

Figure 3-1 The images captured by the microscope for 100x magnification using the 1um green microspheres

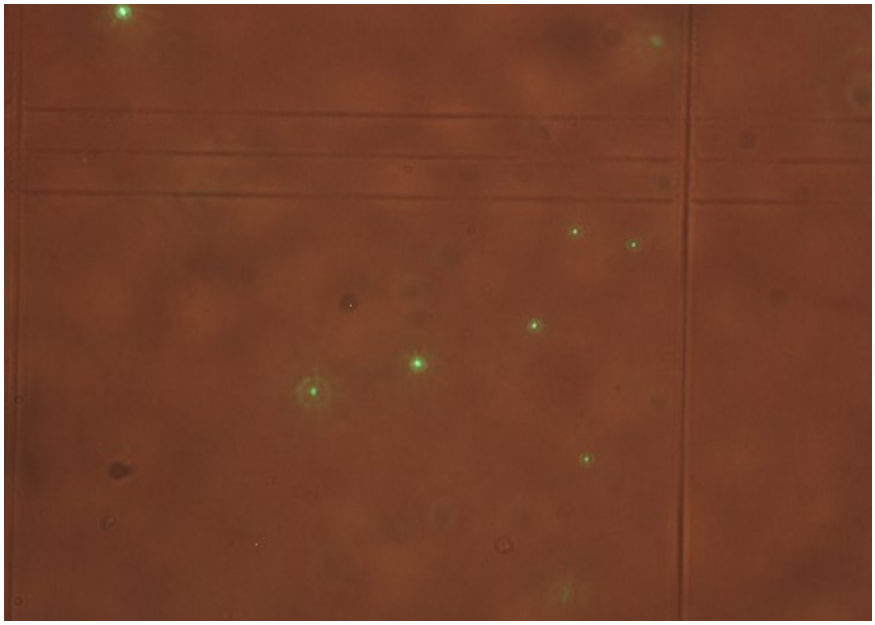

Figure 3-2 The images captured by the microscope for 400x magnification using the 1 um yellow-green microspheres.

Figure 3-3 shows the same microspheres at 100x magnification, but this time with 200 mg/L of sediment present in the solution. Similar to the previous image (Figure 3-1), it is difficult to visualize the microspheres at this magnification and also difficult to distinguish between the sediment and microspheres in some cases.

Figure 3-3 The images captured by the microscope for 100 x magnification using the green microspheres with 200 mg/L sediment added to the sample.

In an attempt to improve upon visualization of the microspheres with the current microscope capabilities, the 2um red microsphere was trialed at the same concentration as that of the green microsphere presented in Figures 3-1 to 3-3. The red microsphere is illuminated at a different wavelength (see section 2-5) and is twice the diameter of the green microsphere. As shown in Figure 3-4, at 100x magnification, the red microsphere is clearer than that shown for the green microspheres, likely due to the larger size and slightly different wavelength used.

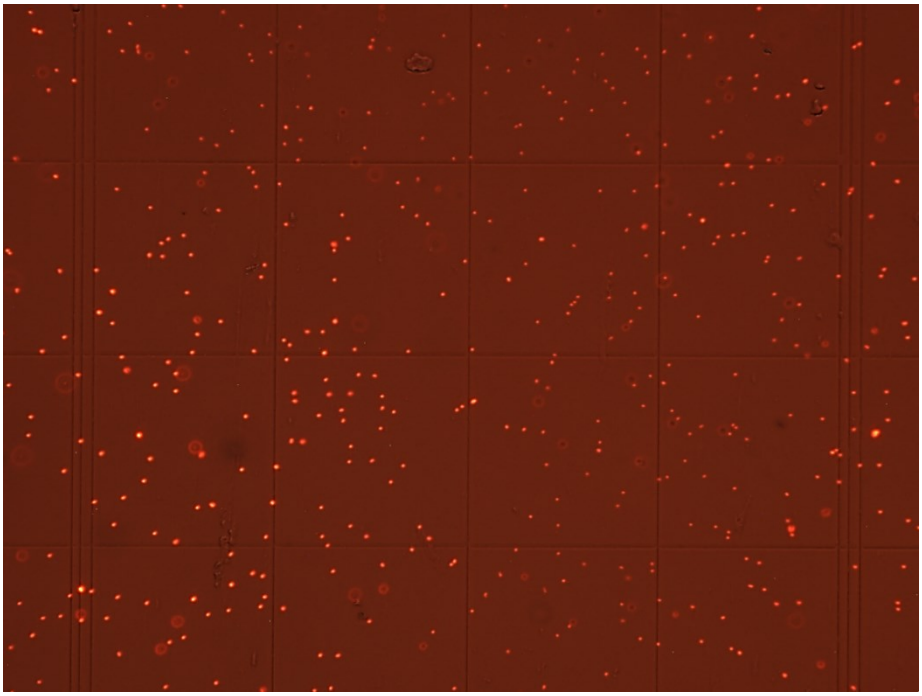

Figure 3-4 The images captured by the microscope for 100x magnification using the red microspheres.

Figure 3-5 shows the same red microsphere at the same concentration, with 200 mg/L of sediment added to the samples using a 100x magnification. The sediment and microspheres are clear and distinguishable from each other for counting purposes. This visualization provided some confidence in the ability to count the microspheres in the presence of sediment in the samples.

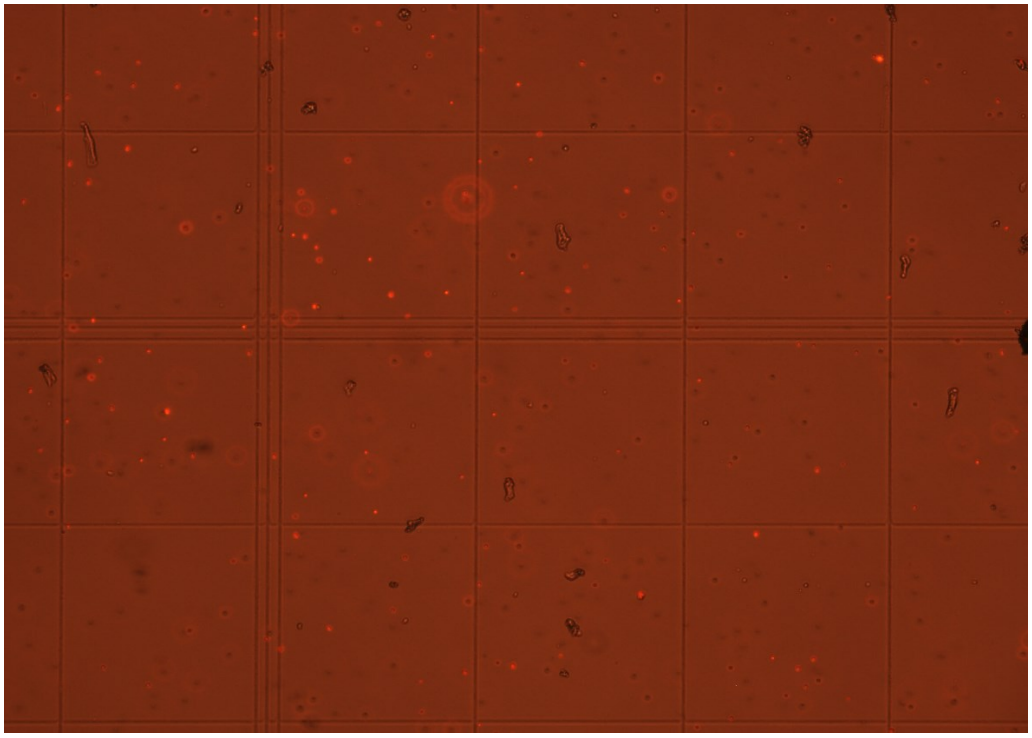

Figure 3-5 The images captured by the microscope for 100 x magnification using the red microspheres with 200 mg/L sediment added to the sample.

3.2 Quantification of Microspheres Using the Optical Microscope

After gaining some confidence in the ability to visualize the microspheres under the microscope and being able to properly distinguish between the microspheres and sediment during imaging, it was necessary to evaluate the ability to detect microspheres in solution, as well as to evaluate the reproducibility of the method. To accomplish this, ten separate 2µl-samples were obtained from a stock solution with a known concentration of red microspheres (460 particles/uL) and each placed on a separate counting slide under the microscope. Each of the 10 slides were then imaged under 100x magnification. The counting process involved counting the number of microspheres separately for each small square and then averaging the number of microspheres for each square. Approximately 8 to 12 squares were used in

the counting process. The average count per slide was then multiplied by 256 (the number of squares) to obtain the total amount of microspheres in the 2uL sample taken from the stock solution. The tests were repeated with sediment added to the stock solution at sediment concentrations of 200 mg/L, 300 mg/L, and 400 mg/L.

Tables 3-1 and 3-2 show the counting results from microscopic images for the samples without sediment (Table 3-1) and with sediment (Table 3-2). Ten measurements were done for ten different samples from the stock solution (Table 3-2) and the stock solution plus sediment (Table 3-3).

Table 3-1 Microsphere counts/ 1 uL (no sediment present)

Sample	Microspheres average counts/square	Microsphere counts/ 2 µl	Microsphere counts/ 1 µl
1	20	5197	2598
2	24	6144	3072
3	21	5312	2656
4	21	5453	2726
5	20	5069	2534
6	18	4685	2342
7	21	5325	2662
8	20	5222	2611
9	20	5069	2534
10	19	4838	2419
Average			2617

Table 3-2 Microsphere counts/1 uL (sediment added with TSS of 200, 300, and 400 mg/l)

Samples	Microspheres average counts/square			Microsphere counts/ 1 μL		
	Sediment added (200 mg/l)	Sediment added (300 mg/l)	Sediment added (400 mg/l)	Sediment added (200 mg/l)	Sediment added (300 mg/l)	Sediment added (400 mg/l)
1	13	26	14	1638	3379	1856
2	14	22	20	1741	2829	2620
3	23	18	20	2944	2291	2624
4	14	20	19	1856	2509	2394
5	29	22	20	3712	2838	2620
6	22	23	17	2842	2948	2176
7	20	30	17	2611	3814	2176
8	20	26	26	2624	3379	3379
9	25	19	20	3162	2401	2620
10	19	27	22	2406	3482	2842
Average	20	23	20	2554	2987	2531

3.3 Data Distributions and Normality

Figures 3-6 to 3-9 present the normality test diagrams of microsphere counting results compiled in Tables 3-1 and 3-2. Normality diagrams plotted in Minitab 21.2 are histogram types used in statistical analysis to assess the distribution of data and to check for normality (Minitab, LLC., 2021). The normality diagram assesses whether the dataset follows a normal distribution. In the normality diagram, the data points are plotted against the expected values of a normal distribution. It is shown that the data points fall along a straight line, so the dataset is approximately normally distributed.

As shown in Figures 3-6 to 3-9, the mean values for microsphere counts are 2617, 2554, 2987, and 2531, the standard deviations are 197.5, 663.5, 510.1, and 418.3, and the total number of data points in each dataset is 10. In addition, Figure 3-6 to 3-9 shows that the

Anderson-Darling (AD) are 0.460, 0.241, 0.278, and 0.389, and P-values are 0.204, 0.697, 0.569, and 0.314. In general, in an AD normality test, smaller values indicate a better fit between the sample distribution. As a general rule of thumb, AD values less than 1 indicates a good fit, while a value greater than 2 indicates a poor fit. However, it's important to note that these values are only suggestions and not universally accepted standards. Because there is no fixed cutoff value that universally indicates a good fit since the appropriate threshold depends on factors such as the sample size and the level of significance (Razali and Wah, 2011). If the p-value is less than the chosen level of significance (0.05), this would indicate that the data do not follow a normal distribution. The normality plots and statistics suggest that the experimental data is normally distributed which allows some statistical hypothesis tests to be performed on the data to assess if there are any differences.

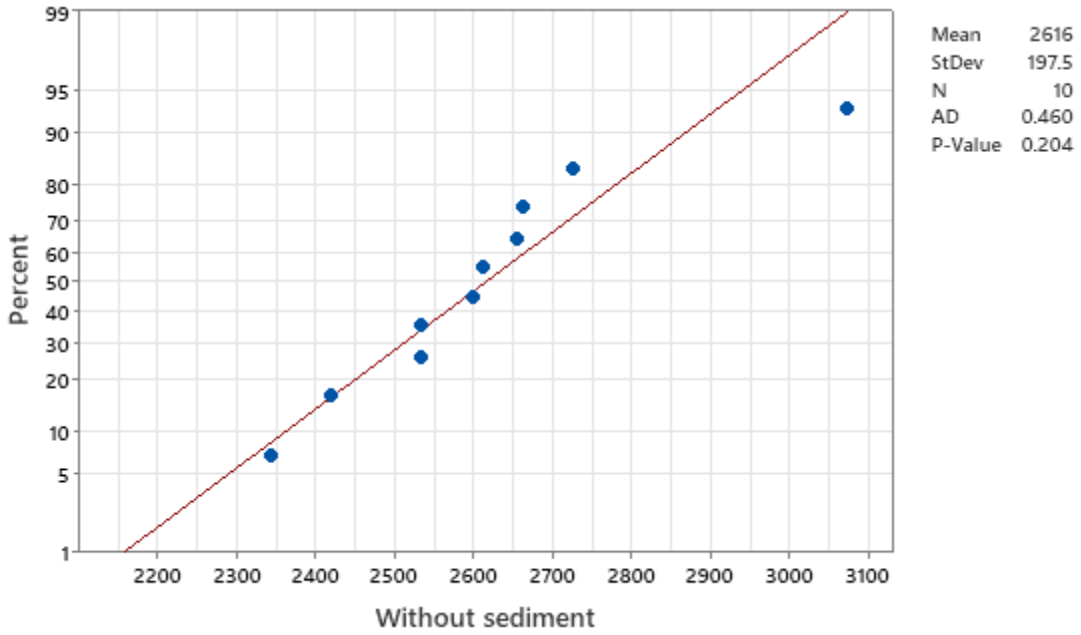

Figure 3-6 Normality test plot of microsphere counts/ul of microsphere solution without sediment

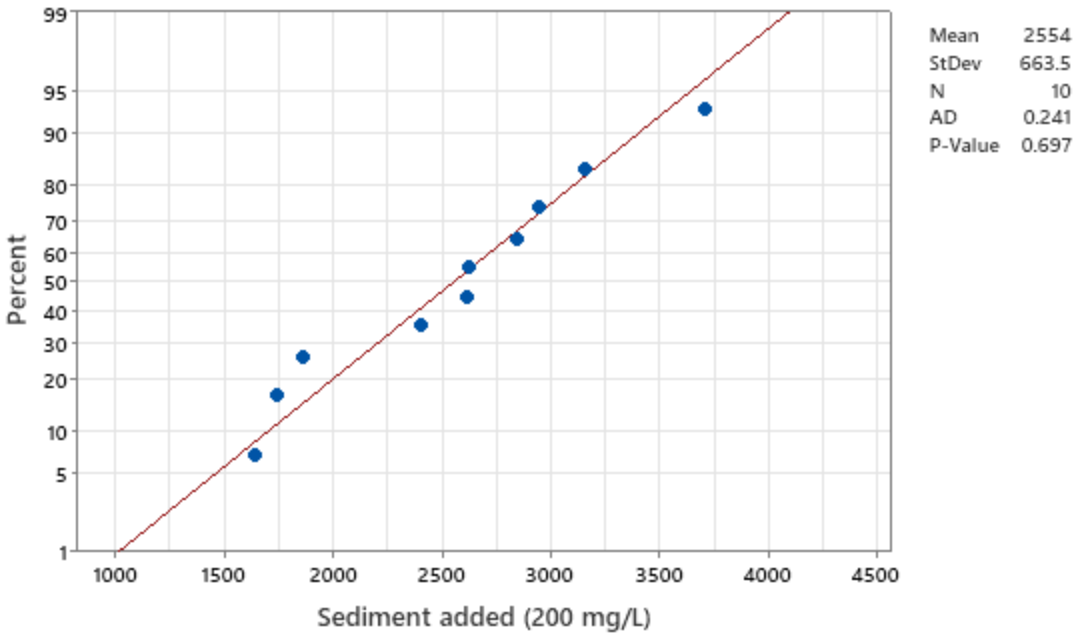

Figure 3-7 Normality test plot of microsphere counts/ul of microsphere solution plus sediment (200 mg/l)

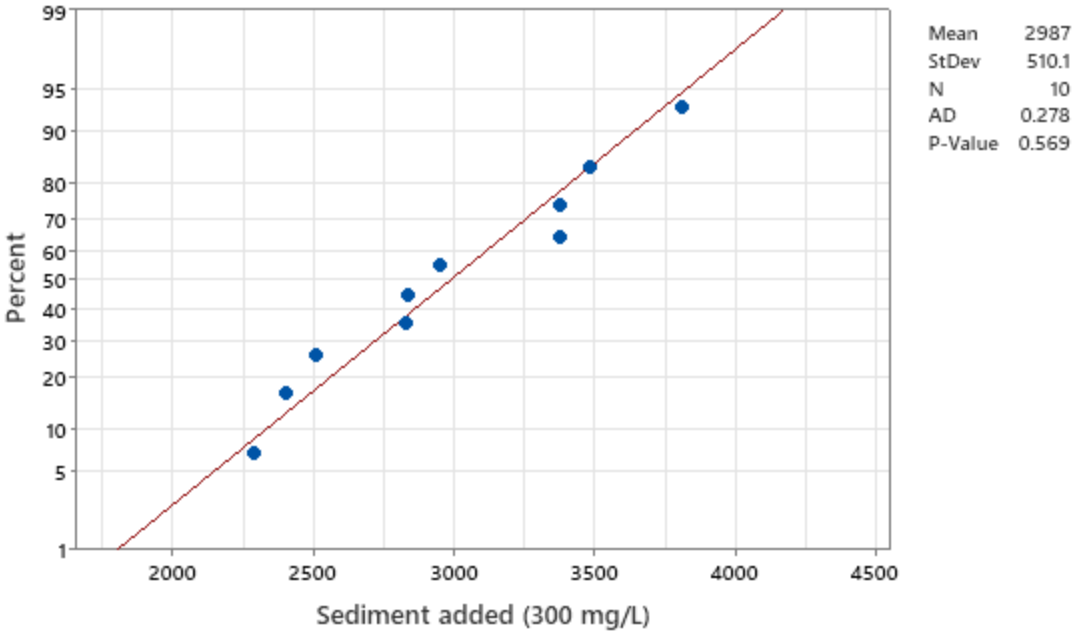

Figure 3-8 Normality test plot of microsphere counts/ul of microsphere solution plus sediment (300 gr/l)

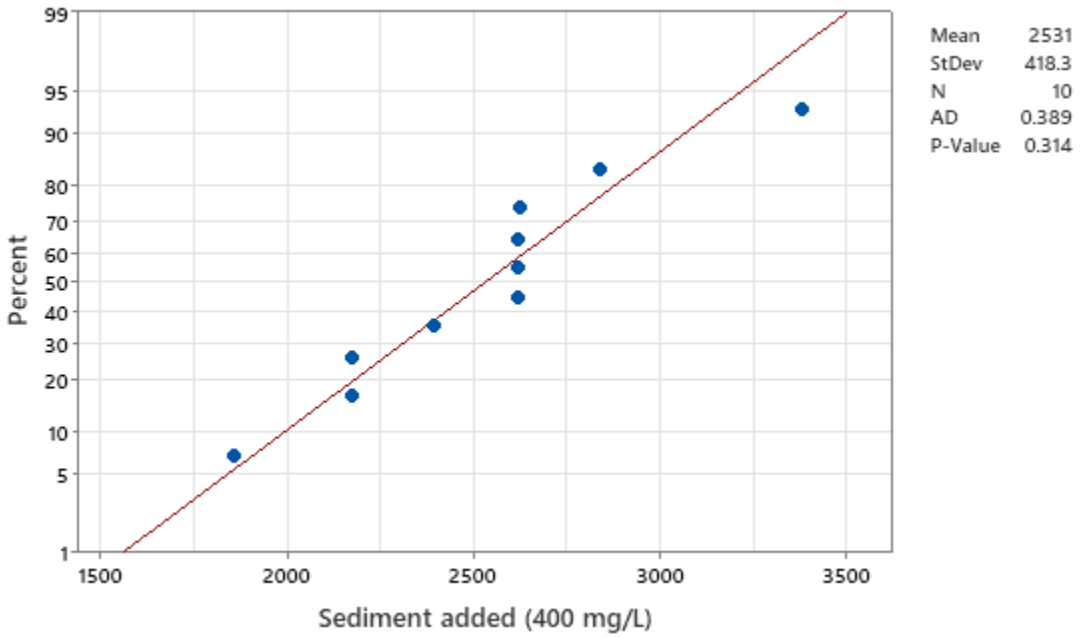

Figure 3-9 Normality test plot of microsphere counts/ul of microsphere solution plus sediment (400 mg/l)

T-tests were performed to assess where there was any effect of the sediment on the quantification of microspheres in solution. In this thesis, the t-test was used to compare the mean value of the microsphere concentration with no sediment in solutions to the mean values of the microsphere concentration with sediments (i.e. three separate tests). This was performed in Microsoft Excel, the results of which are reported in Table 3-3.

Table 3-3 T-test Results for Comparing Mean Sample Concentrations (no sediment vs. sediment in sample)

Test	Microsphere Concentrations (#/ul), No Sediment	Microsphere Concentrations (#/ul), 200 mg/L of Sediment	Microsphere Concentrations (#/ul), 300 mg/L of Sediment	Microsphere Concentrations (#/ul), 400 mg/L of Sediment
Mean	2616	2554	2987	2530
Variance	39013	440193	260175	174192
Observations	10	10	10	10
Tstat	-	0.28	2.15	0.58
T-Critical (two-tail, 0.05)	-	2.2	2.2	2.2
Outcome		No significant difference	No significant difference	No significant difference

These results indicate that within a 0.05 significance level, there is no significant difference in microsphere concentrations when up to 400 mg/L of sediment is present.

3.4 Discussion

This chapter has worked at developing some confidence in the ability to visualize and quantify the microspheres in solution using the optical microscope. Initial attempts with a 1-um, yellow green microsphere at 100x and 400x magnification were not satisfactory. However, the 2-um red microsphere showed promise in visualization at both magnifications, even in the presence of sediment. The quantification process was validated with some simple statistical analyses which showed that there was no significant difference between samples without and with sediment. This confidence in the experimental methods allowed progression to the dewatering test method development work present in the follow chapter.

4 Dewatering Test Results and Discussions

This chapter incorporates the visualization and quantification methods presented in the previous chapter to perform the various dewatering tests discussed in Section 2.7.

4.1 Filtration Rate

For each of the tests listed in Table 2-4, the time it took for each 250 ml sample to be collected was measured. The results for each test are presented in Figures 4-1 to 4-3. For all six tests, at each step, there is a notable decrease in flow through the filter cake as the experiment progresses, indicating both a decrease in the filtration rate at early stages of the tests but also due to a decrease in total head on the filter cake as the test progressed. Specifically, the first 250 ml samples were obtained relatively quickly, irrespective of the test or step, whereas the subsequent 250 ml samples took progressively longer to collect. This pattern was observed consistently across all tests. The larger thickness of the filter cakes and its effect on flow can be observed by comparing the 100 g test to the 200 g and 300 g tests for step 1 in Figure 4-1.

The following observations were made from Figure 4-1. Firstly, as the quantity of soil mixture 1 increased from 100 g to 300 g, the time taken for each step to drain became progressively longer. Similarly, for soil mixture 2, an increase in the amount of soil mixture from 100 g to 300 g resulted in a progressive increase in the time taken for each step to drain. When comparing soil mixtures 1 and 2 at 100 g and 300 g revealed that the finer grained soil (soil 1) took more time to drain than the coarser soil (soil 2). However, at 200 g, the finer soil (soil 1) took less time to drain compared to the coarser soil (soil 2), which is not

expected. It is likely that there was some disturbance to the filter cake created for soil mixture 1 during step 1 when the slurry was poured in the upper chamber, which resulted in these slightly higher flows. Similar trends for step 2 and step 3 (Figures 4-2 and 4-3) were observed. The higher rate of filtration of the 200 g soil mixture 1 relative to soil mixture 2 was also present in these steps.

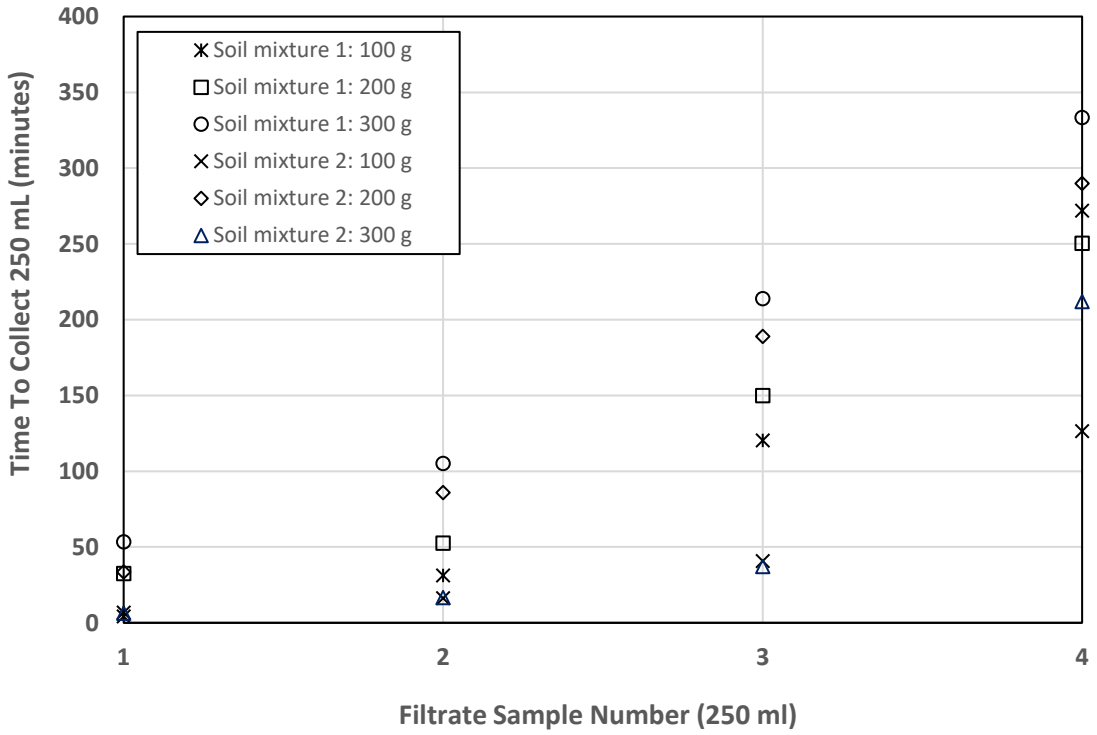

Figure 4-1 Filtration Flow Rates – Step 1: Filter cake development with each sediment concentration and soil mixture type

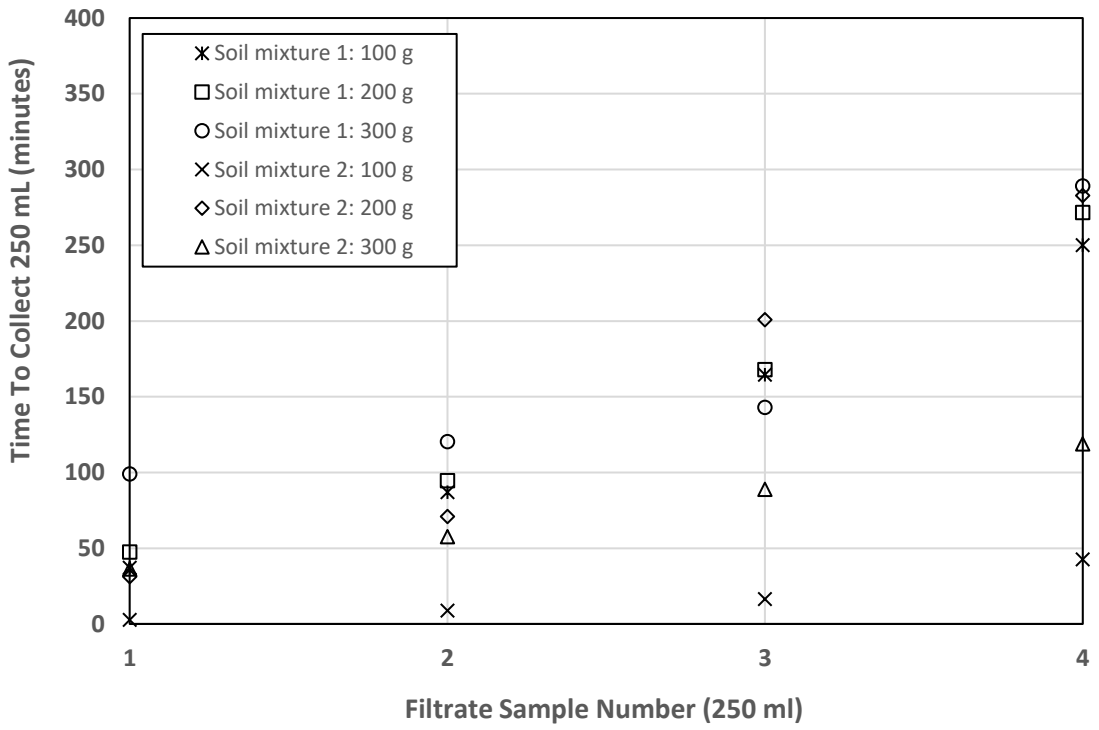

Figure 4-2 Filtration Rate – Step 2: Microsphere solution dewatering with each sediment concentration and soil mixture type

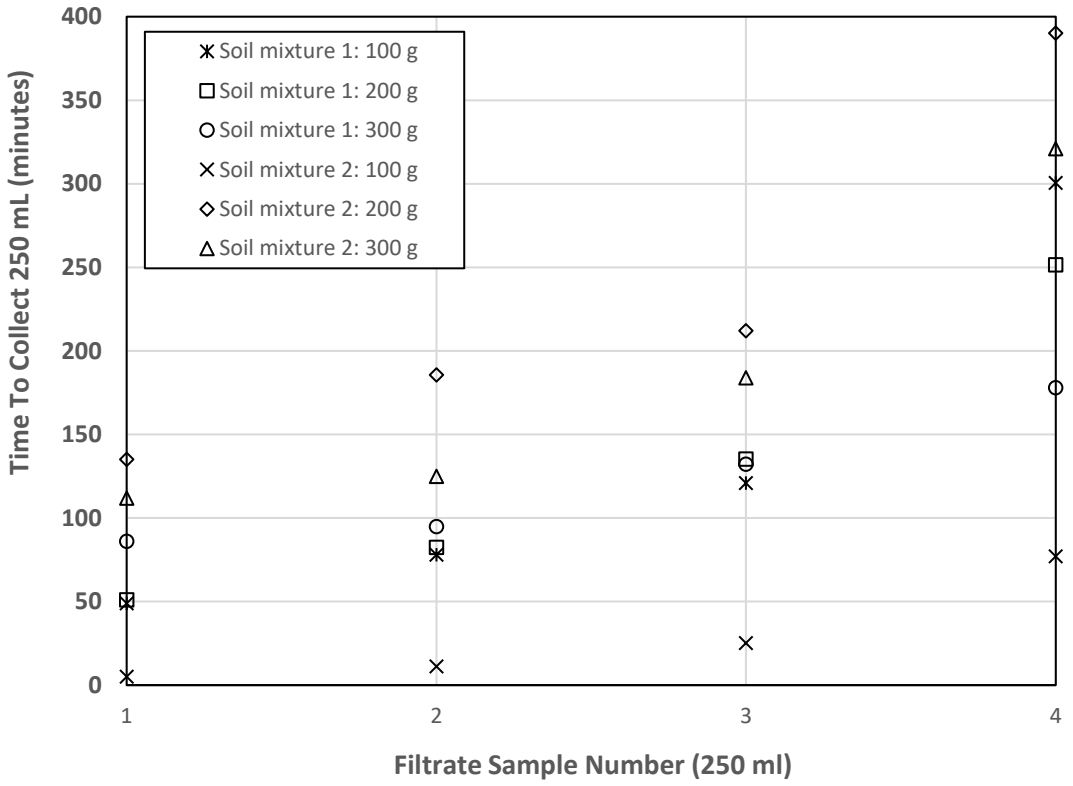

Figure 4-3 Filtration Rate – Step 3: Water filtration with each sediment concentration and soil mixture type

4.2 Total Suspended Solids (TSS)

The TSS results for each 250 ml from each step of each test are shown in Figures 4-4 to 4-6. As anticipated, the TSS values are highest during the initial 250 ml of sampling for any test. The TSS results for the first filtrate samples obtained from the filter cake development tests (Step 1) were significantly higher than those collected from the microsphere solution dewatering tests (Step 2) and water filtration tests (Step 3). However, there was a notable exception for the 100 g test that used 100 grams of soil mixture 2 for all steps.

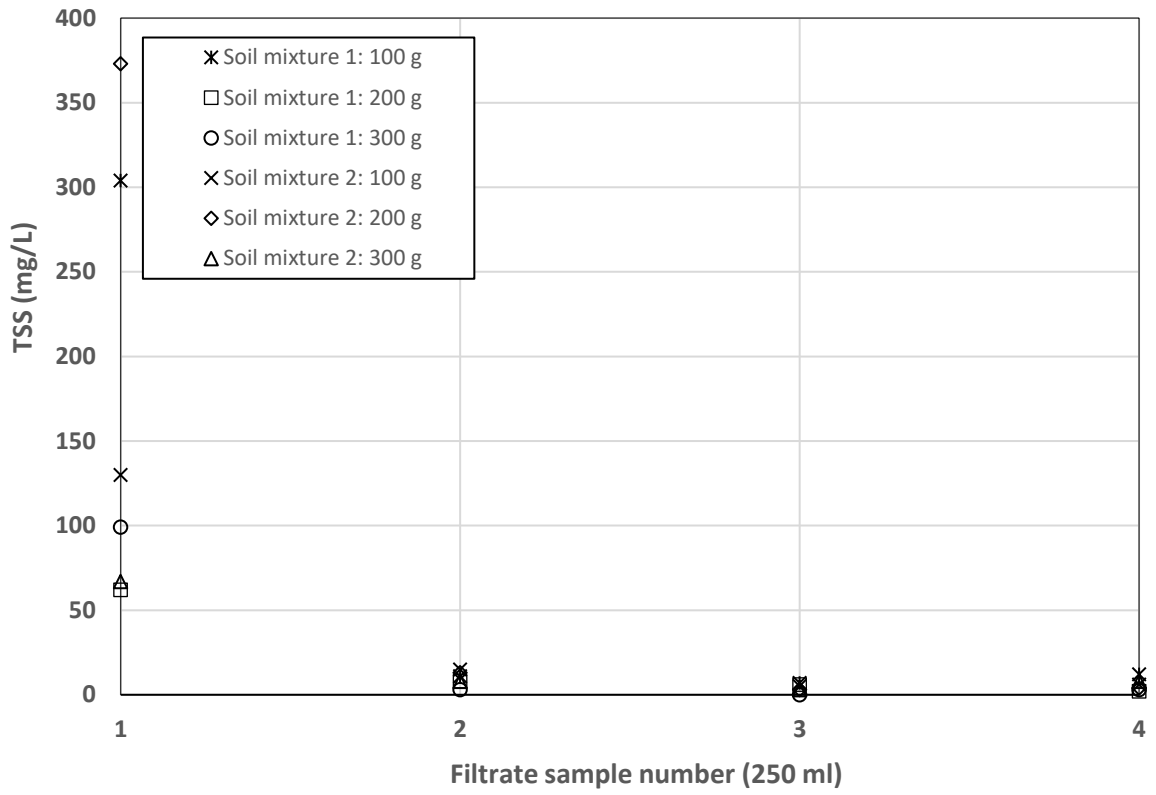

Figure 4-4 TSS Measurement (Filter cake development tests)

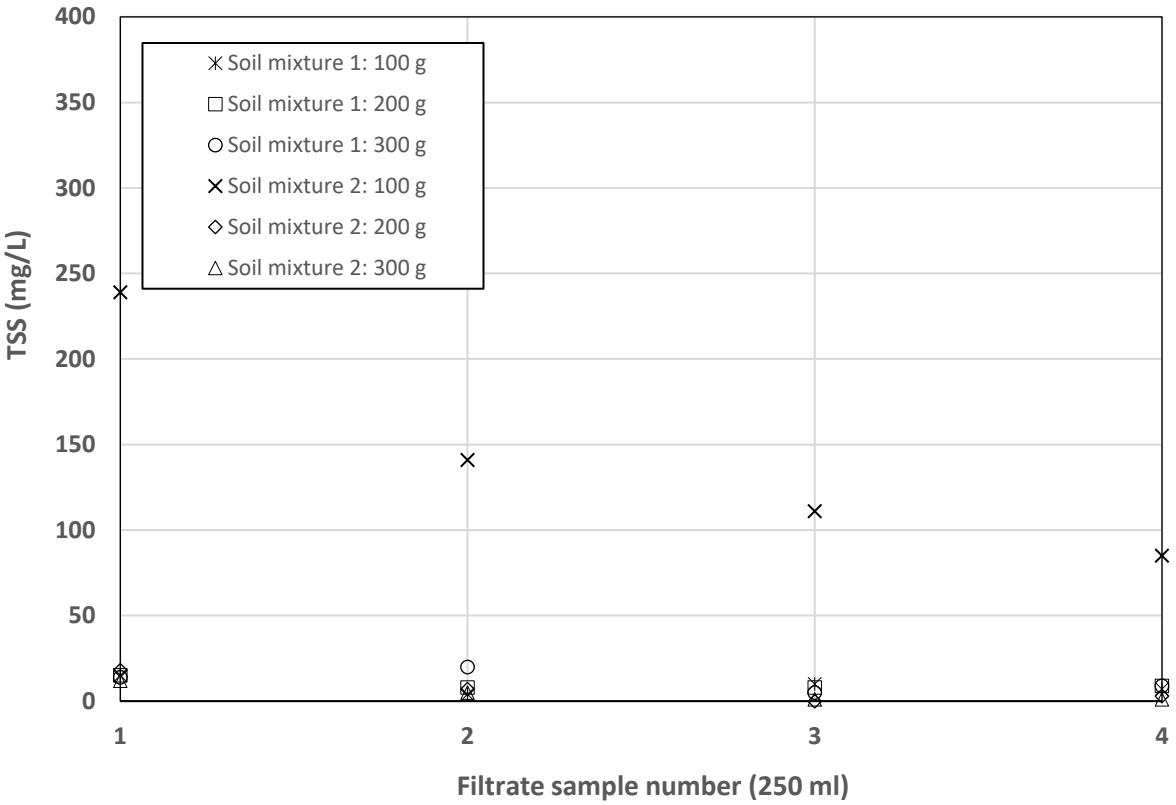

Figure 4-5 TSS Measurement (Microsphere solution dewatering tests)

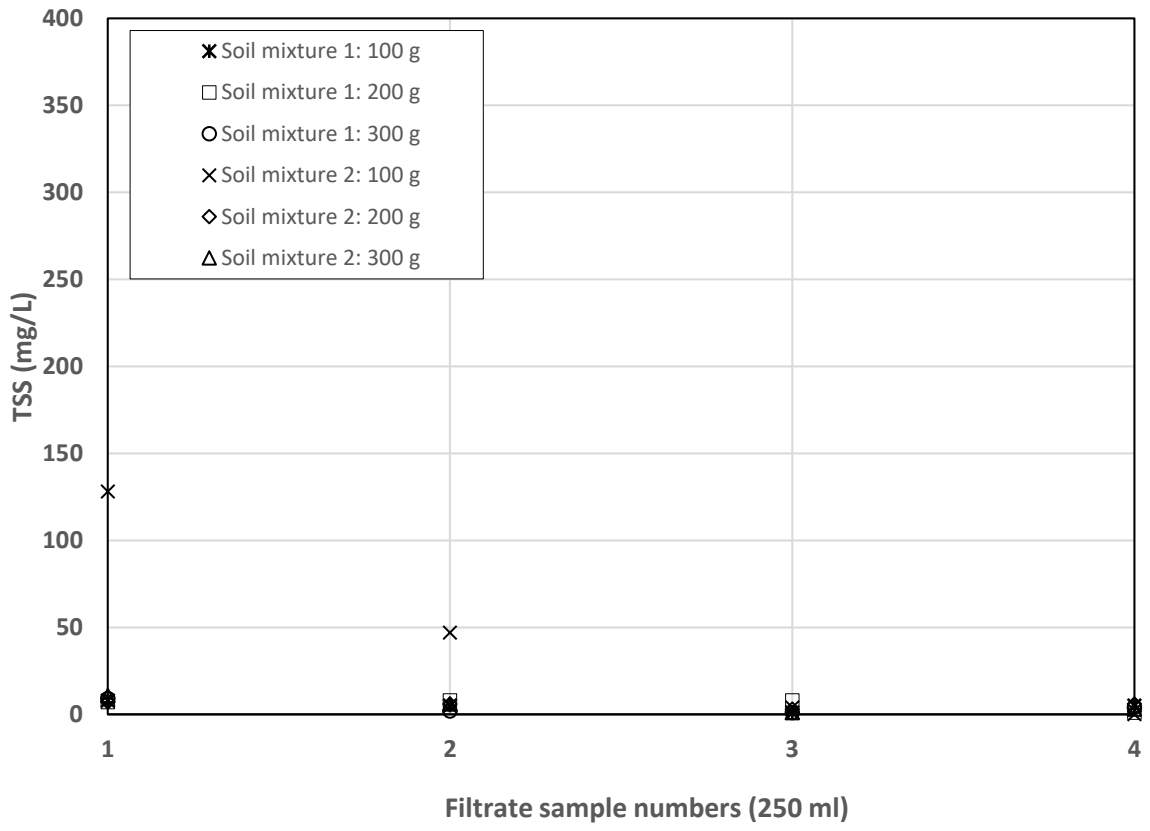

Figure 4-6 TSS Measurement (Water filtration tests)

4.3 Microsphere Concentration

4.3.1 Filtrate Samples From Step 2 Tests

Figures 4-7 (Soil mixture 1) and 4-8 (Soil mixture 2) show the mean microsphere counts (from ten, 2-µl samples) with standard deviations (error bars). Similar to the TSS trends in the previous section, the concentration of microspheres in the filtrate samples generally decreases with each subsequent 250 ml sample. Furthermore, it was generally observed that as the filter cake thickness increased, the number of microspheres decreased or stayed the same.

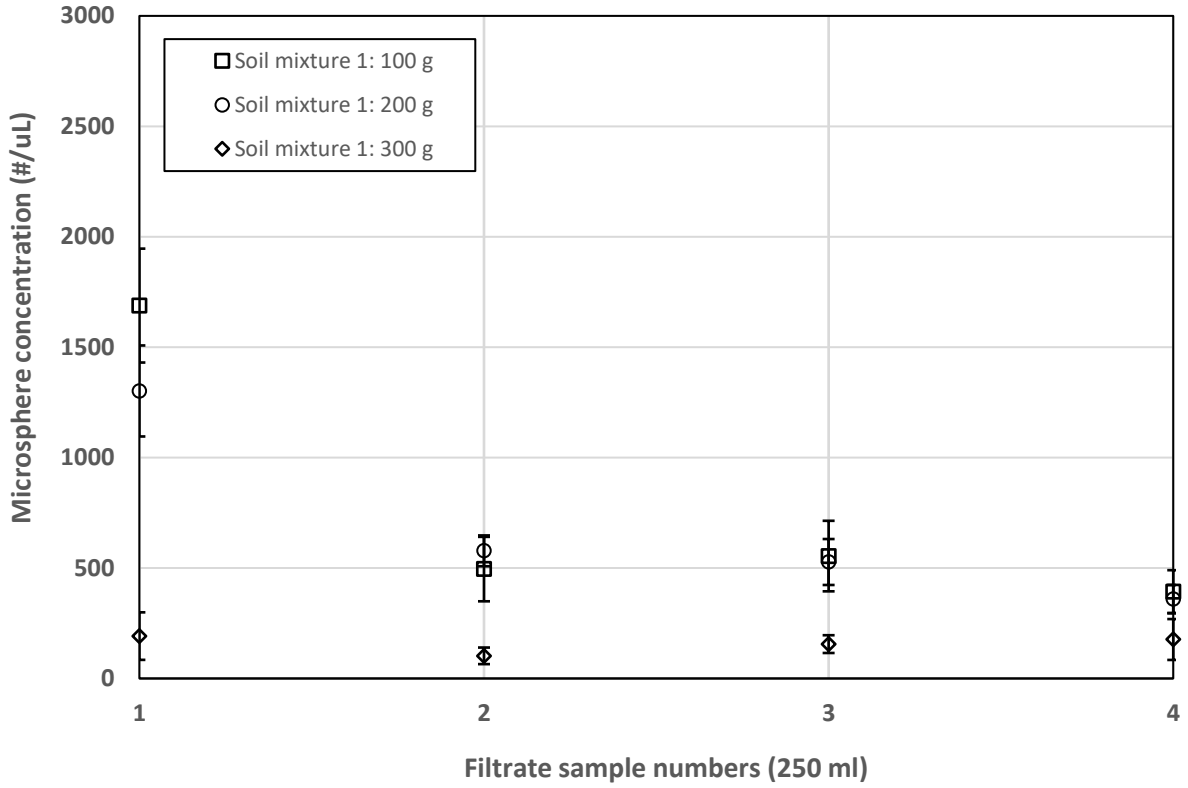

Figure 4-7 Microsphere counts/uL (Microsphere solution dewatering tests-Soil mixture 1). Symbols represent mean values, error bars represent one standard deviation from the mean.

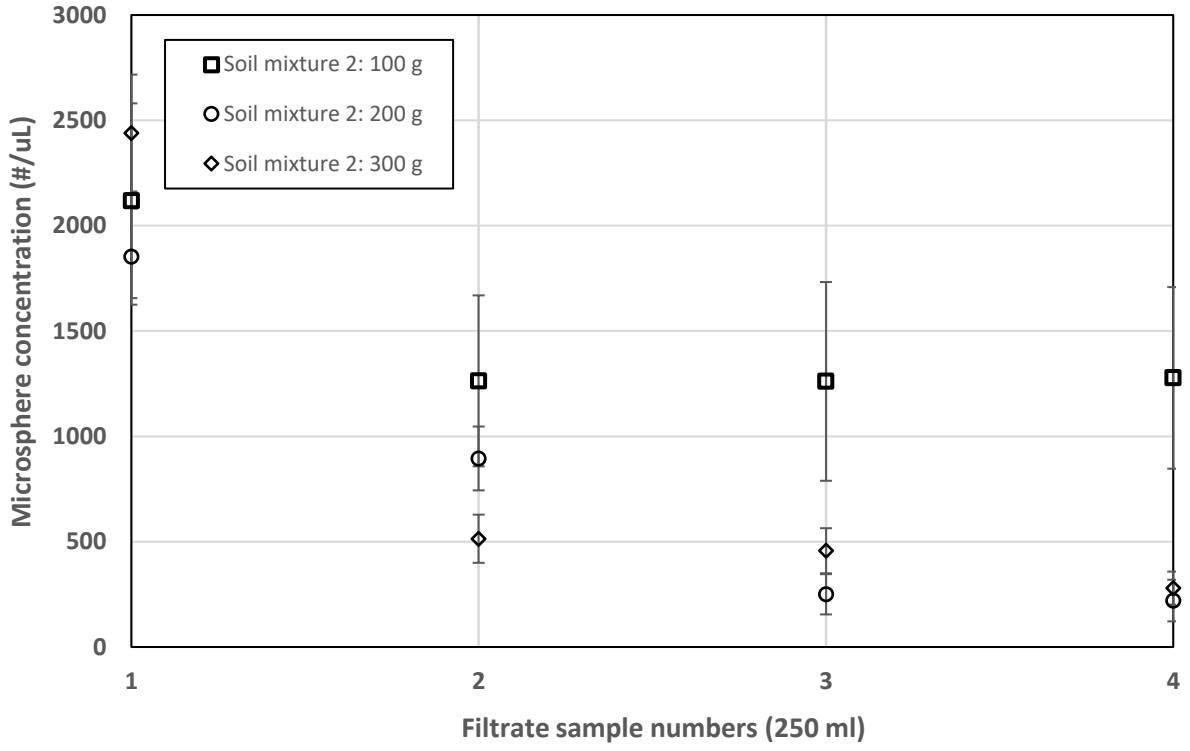

Figure 4-8 Microsphere counts/uL (Microsphere solution dewatering tests-Soil mixture 2). Symbols represent mean values, error bars represent one standard deviation from the mean.

The microsphere counts for the tests conducted with soil mixture 2 were generally higher than those of the finer soil mixture 1. The exception to this is that of soil mixture 1, 100g. As noted in the previous section, this trend is consistent with TSS results which is encouraging as it provides some confidence that microspheres are following similar trends as TSS.

4.3.2 Filtrate Samples From Step 3 Tests

Figures 4-9 and 4-10 offer insight into the average microsphere counts obtained from water filtration through filter cakes constructed from slurry filtration. The results indicate that, as

anticipated, there was a decline in microsphere counts over time for each test. This is likely due to some of the microspheres present in the filter cake being more easily detached than those microspheres released in subsequent 250 ml samples due to lesser amounts of seepage forces on the filter as the test progressed. As the filter cake thickness increased, the microsphere counts did not necessarily decrease; there are some fluctuations for soil mixture 1 in Figure 4-9 and for soil mixture 2 in Figure 4-10. Tables 4-1 and 4-2 show the t-test results done for the data shown on Figures 4-9 and 4-10. As shown on Tables 4-1 and 4-2, there is not actually no significant difference between microsphere concentration of filtrates collected from the water filtration tests (step 3) when compared to the 100 g size for each soil mixture.

When comparing Step 2 data to Step 3 data, it is apparent that the microsphere counts of the filtrates gathered from the microsphere solution dewatering tests (Figures 4-7 and 4-8) are greater than those from the water filtration tests (Figures 4-9 and 4-10). Furthermore, the data suggests that the microsphere concentration of the samples collected from the tests utilizing the second soil mixture is higher than those from the corresponding tests employing the first soil mixture. However, there are two exceptions: the second 250-ml filtrate sample collected from 200 g filter cake, and the fourth 250-ml filtrate sample collected from 300 g filter cake.

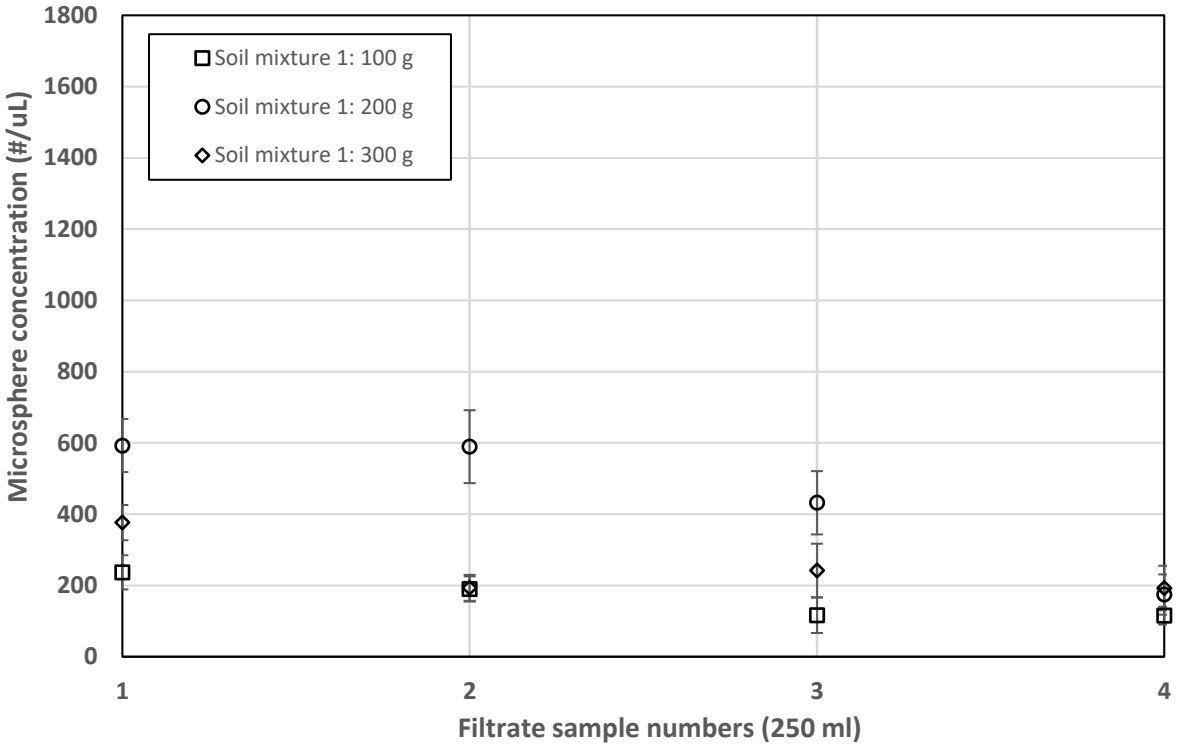

Figure 4-9 Microsphere counts/uL (Water filtration tests-Soil mixture 1). Symbols represent mean values, error bars represent one standard deviation from the mean.

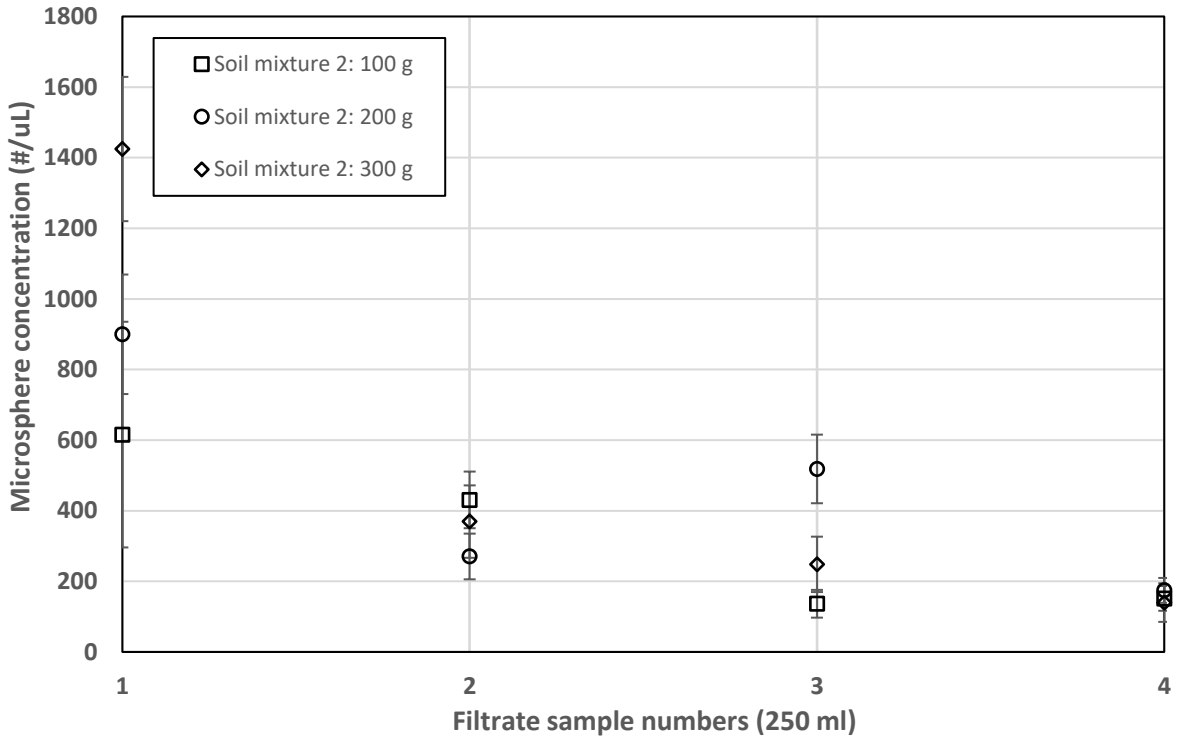

Figure 4-10 Microsphere counts/uL (Water filtration tests-Soil mixture 2). Symbols represent mean values, error bars represent one standard deviation from the mean.

Table 4-1 T-test Results for Comparing Mean Sample Concentrations (Soil mixture 1: 100 g vs. 200 g and 100 g vs. 300 g)

Test	Microsphere Concentrations (#/ul), Water filtration test (soil mixture 1: 100 g)	Microsphere Concentrations (#/ul), Water filtration test (soil mixture 1: 200 g)	Microsphere Concentrations (#/ul), Water filtration test (soil mixture 1: 300 g)
Mean	165	447	251
Variance	3544	38666	7503.675067
Observations	4	4	4
Tstat	-	2.75	1.65
T-Critical (two-tail, 0.05)	-	2.78	2.57
Outcome		No significant difference	No significant difference

Table 4-2 T-test Results for Comparing Mean Sample Concentrations (Soil mixture 2: 100 g vs. 200 g and 100 g vs. 300 g)

Test	Microsphere Concentrations (#/ul), Water filtration test (soil mixture 2: 100 g)	Microsphere Concentrations (#/ul), Water filtration test (soil mixture 2: 200 g)	Microsphere Concentrations (#/ul), Water filtration test (soil mixture 2: 300 g)
Mean	334	466	545
Variance	53655	104731	352308
Observations	4	4	4
Tstat	-	0.66	0.66
T-Critical (two-tail, 0.05)	-	2.57	2.78
Outcome		No significant difference	No significant difference

4.4 Filter Cake Efficiency

The results presented in Figure 4-11 depict the percentage of initial microspheres that were attached and then detached from the filter cake during the tests. The following formulas were used to calculate these percentages:

$$\% \text{ Attached} = (y-x)*100/y \quad (4\text{-}1)$$

$$\%\text{Detached} = (z)*100/y \quad (4\text{-}2)$$

Where:

x = number of microspheres measured in 1000 mL of effluent from Step 2

y = number of microspheres initially added to filter cake at beginning of Step 2

z = number of microspheres measured in 1000 mL of effluent from Step 3

Specifically, in step 2 of the experiment, microspheres became attached to the filter cake, while others passed through the filter cake. In step 3, microspheres became detached as

water filtration occurred in step 3. The graphical data illustrates that soil mixture 1 exhibits more efficiency in trapping microspheres, with 70.7%, 74.1%, and 94.1% of the initial microspheres attaching to the filter cakes composed of 100 g, 200 g, and 300 g of soil mixture 1, respectively. In contrast, the equivalent amounts for soil mixture 2 are 44.6%, 69.9%, and 65.5%.

Moreover, the results indicate that soil mixture 2 experienced more detachment than soil mixture 1, due to grainsize differences. Specifically, 12.5%, 17.4%, and 20.4% of the initial microspheres detached from the filter cakes made of 100 g, 200 g, and 300 g of soil mixture 2, respectively, compared to 6.2%, 16.7%, and 9.4% for the equivalent tests conducted with soil mixture 1.

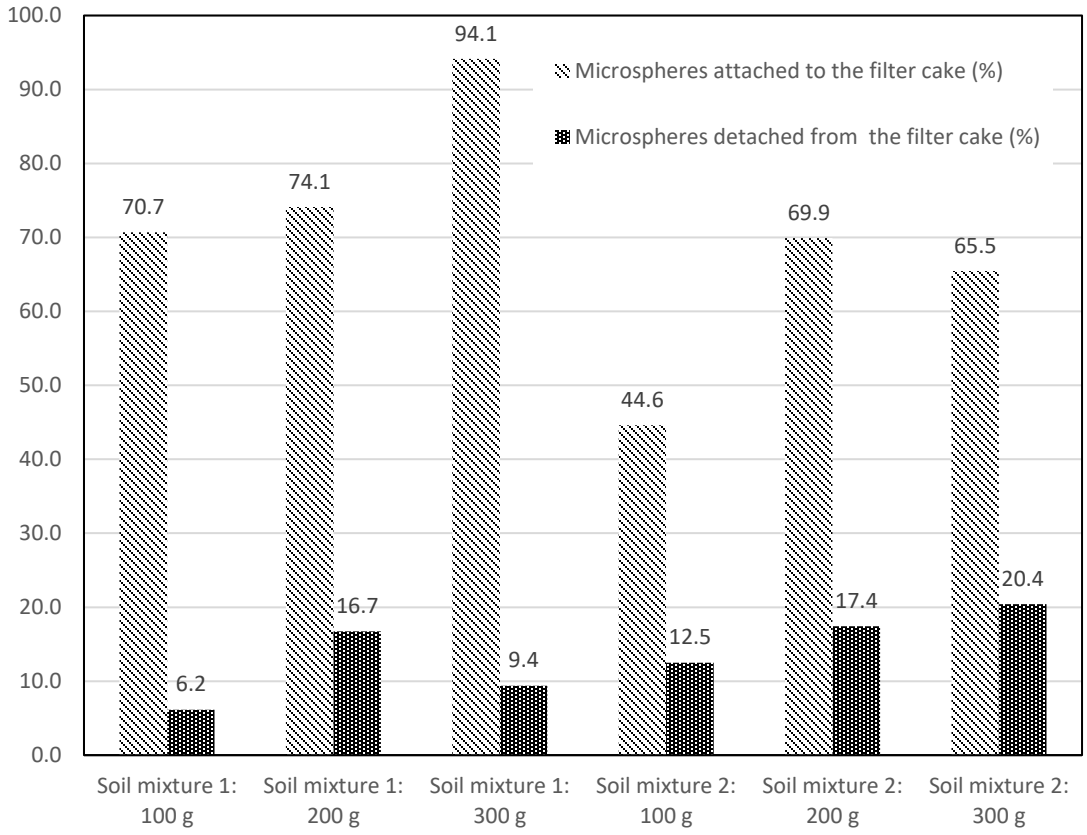

Figure 4-11 Percentage of initial added microspheres attached and detached from filter cakes

4.5 Reproducibility of Dewatering Test Microsphere Measurements

To assess the reproducibility of these types of tests in terms of microsphere measurements, both the 100 g of soil mixture 1 and 200 g of soil mixture 2 were repeated. Microscopic measurements were conducted on the filtrates collected from the microsphere solution dewatering and water filtration tests, with the results presented in Figures 4-12 to 4-15. Symbols denote mean values and error bars the standard deviations. Also shown on these figures are the original test results for these conditions, presented in the previous sections.

Compared to previous tests, the results displayed in Figures 4-12 to 4-15 visually exhibit similarity, suggesting reproducibility.

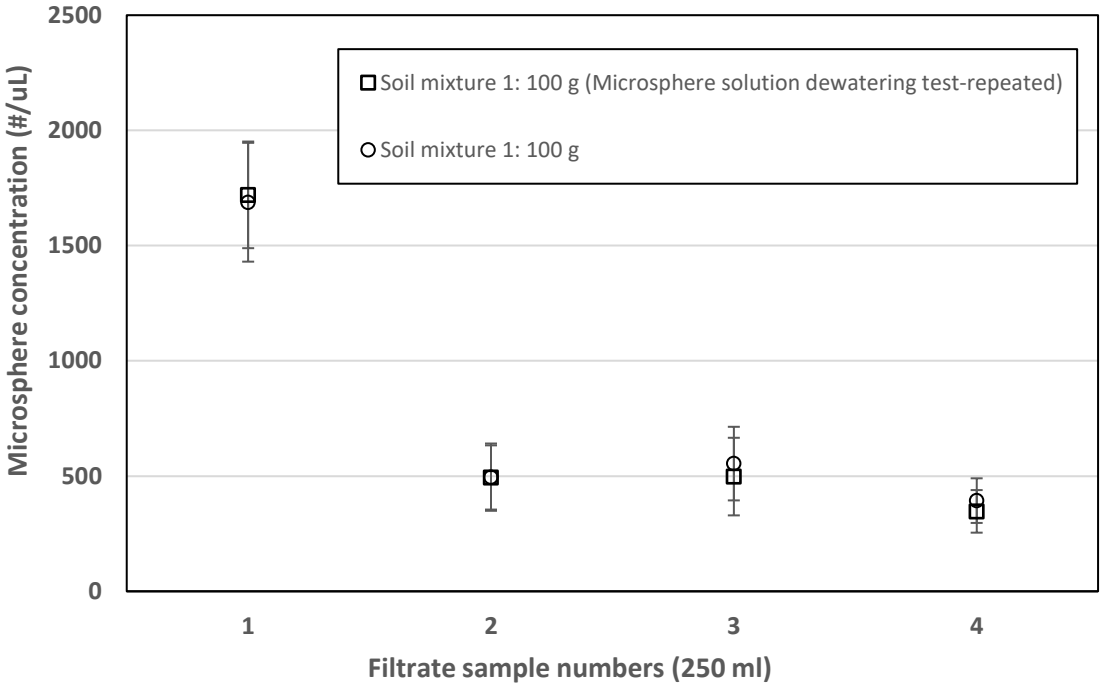

Figure 4-12 Data validation for tests (microsphere solution dewatering tests) done with 100 g of soil mixture 1. Symbols represent mean values, error bars represent one standard deviation from the mean.

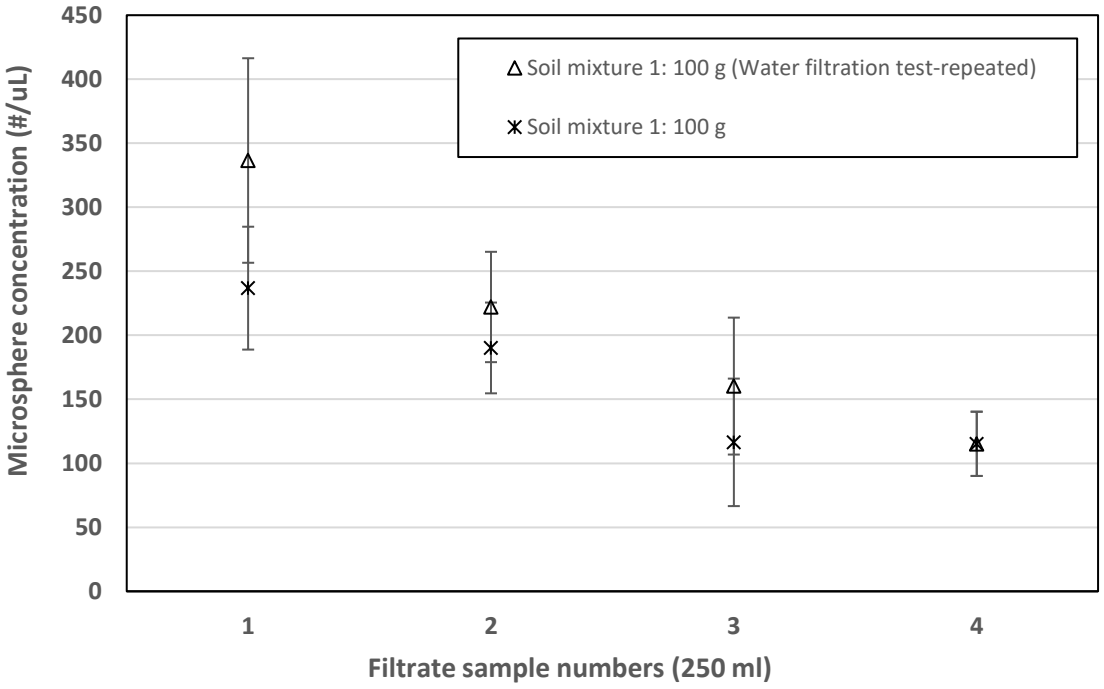

Figure 4-13 Data validation for tests (water filtration tests) done with 100 g of soil mixture 1. Symbols represent mean values, error bars represent one standard deviation from the mean.

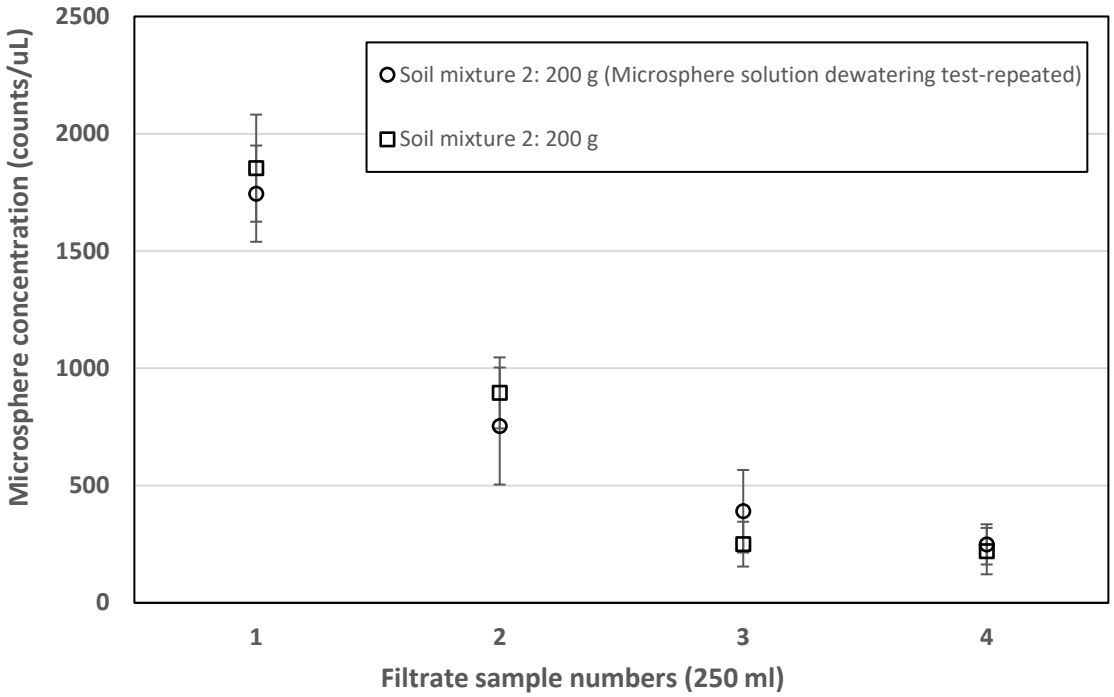

Figure 4-14 Data validation for tests (microsphere solution dewatering tests) done with 200 g of soil mixture 2. Symbols represent mean values, error bars represent one standard deviation from the mean.

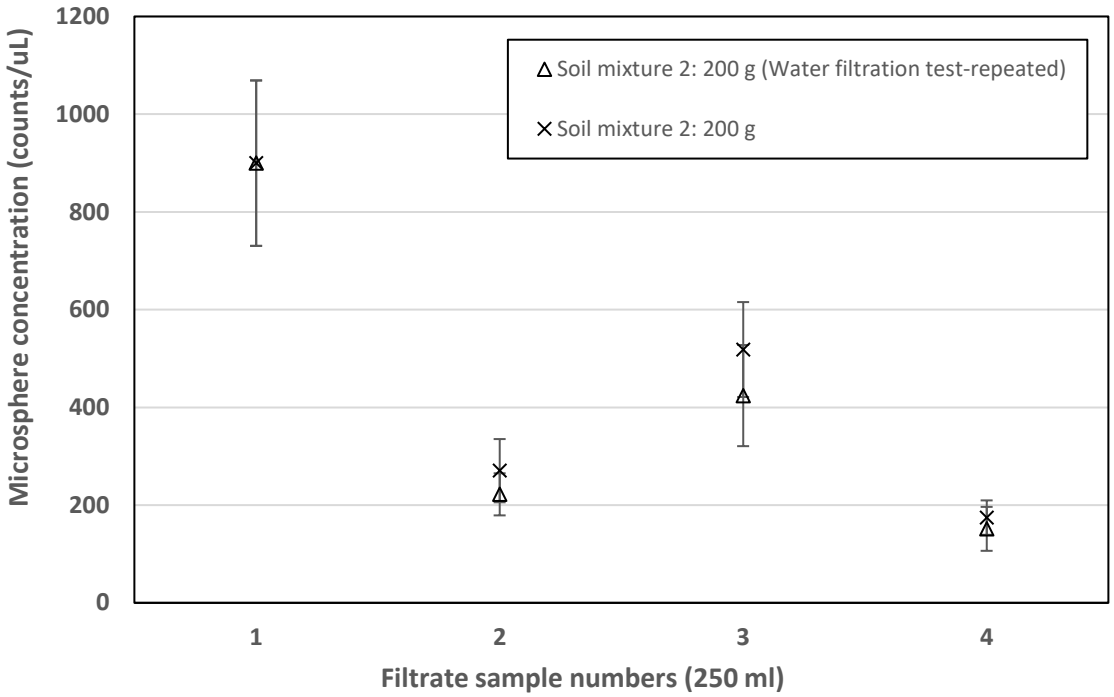

Figure 4-15 Data validation for tests (water filtration tests) done with 200 g of soil mixture 2. Symbols represent mean values, error bars represent one standard deviation from the mean.

To examine this reproducibility further, statistical analyses using t-tests using Microsoft Excel were conducted to examine whether there were statistical differences between the means of the tests performed under the same conditions (Table 4-3). As summarized in this table, there is no significant difference between the original and repeated tests.

Table 4-3 T-test Results for Comparing Mean Sample Concentrations (original tests vs. repeated tests)

Test	Mean	Variance	Observations	Tstat	T-Critical (two-tail, 0.05)	Outcome
Microsphere Concentrations (#/ul), Microsphere solution dewatering test (soil mixture 1: 100 g-original test)	783	368768	4	-	-	
Microsphere Concentrations (#/ul), Microsphere solution dewatering test (soil mixture 1: 100 g-repeated test)	765	410728	4	0.040	2.44	No significant difference
Microsphere Concentrations (#/ul), Water filtration test (soil mixture 1: 100 g-original test)	165	3544	4	-	-	-
Microsphere Concentrations (#/ul), Water filtration test (soil mixture 1: 100 g-repeated test)	208	9190	4	0.778	2.57	No significant difference
Microsphere Concentrations (#/ul), Microsphere solution dewatering test (soil mixture 2: 200 g-original test)	805	585537	4	-	-	-
Microsphere Concentrations (#/ul), Microsphere solution dewatering test (soil mixture 2: 200 g-repeated test)	784	454889	4	0.039	2.45	No significant difference
Microsphere Concentrations (#/ul), Water filtration test (soil mixture 2: 200 g-original test)	466	104731	4	-	-	-
Microsphere Concentrations (#/ul), Water filtration test (soil mixture 2: 200 g-repeated test)	424	113832	4	0.177	2.44	No significant difference

4.6 Post-Test Filter Cake Observations

After each of the six different tests, each filter cake was taken from the dewatering test apparatus for examination. One of the advantages of using microspheres in these types of experiments is not only examining filtrate concentrations but also examining distribution of the microspheres within the filter cakes. This allows additional insight into mechanisms of particle movement through the filter cake. Photos of each of these filter cakes are shown in

Figures 4-16 to 4-18. In these figures, one can see the clear development of the finer grained soil over the coarser grained soil. In some of these photos, one can also see some of the microspheres trapped in the upper portion of the filter cake (i.e., discernible as pink patches). Figure 4-18(b) provides a couple of photos of the filter cake developed using 100 grams of soil mixture 2, which was distinct from soil mixture 1 (Figure 4-18 (a)) in terms of its particle size distribution. As detailed in Table 2-3, the second soil mixture comprised a lesser proportion of fine soil particles, leading to the less cohesive and firm filter cake observed in Figure 4-18 (b).

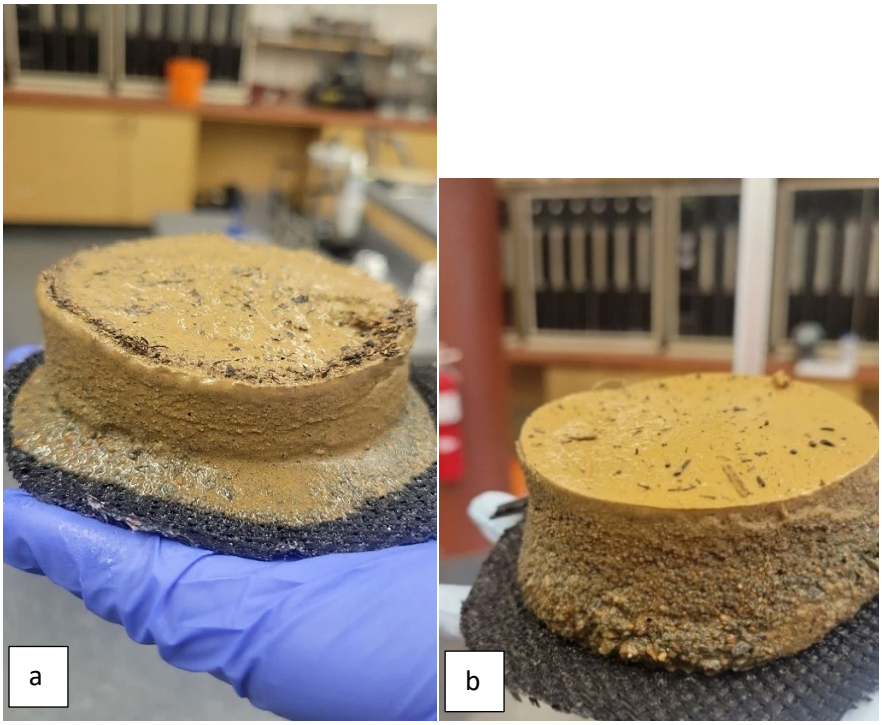

Figure 4-16 Filter cakes developed during 300 g slurry dewatering (a: Soil mixture 1, b: Soil mixture 2)

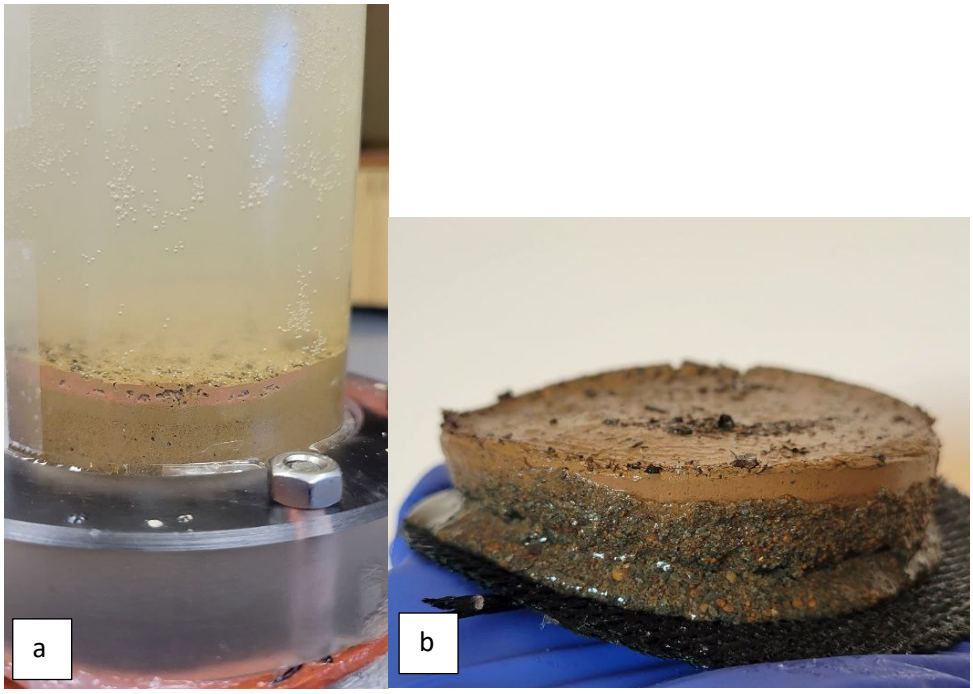

Figure 4-17 Filter cakes developed during 200 g slurry dewatering (a: Soil mixture 1, b: Soil mixture 2)

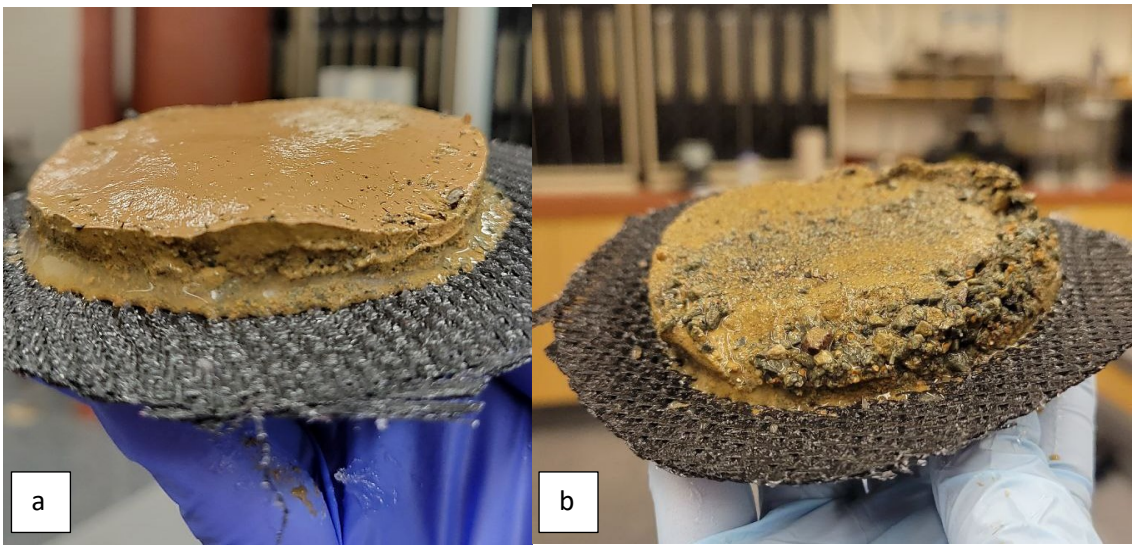

Figure 4-18 Filter cakes developed during 100 g slurry dewatering (a: Soil mixture 1, b: Soil mixture 2)

Three discrete samples were taken from the upper, middle, and bottom layers of each filter cake formed of 200 g of soil mixture 2 to conduct a microscopic examination of the degree of microsphere attachment within the filter cake. The resulting microscopic images, presented in Figures 4-19, 4-20, and 4-21, were obtained at 40x and 100x magnification. The significant accumulation of microspheres in the upper layer of the filter cake is noted in these figures, which primarily consists of fine-grained soil (Figure 4-19). In contrast, the middle layer exhibited comparatively fewer microspheres attached to its surface (Figure 4-20). As expected, the bottom layer, composed primarily of coarse-grained soil, was unable to adsorb microspheres due to its higher porosity (Figure 4-21). These images allow an idea of the mechanisms of particle movement through filter cakes during dewatering to be obtained. It can be inferred that during the microsphere solution dewatering tests the microspheres undergo attachment onto the filter cake, particularly on the uppermost layer. Subsequently, during the water filtration tests, a proportion of these adhered microspheres become detached from the filter cake, particularly from the middle and lower layers, and flow out of the filter cake. This phenomenon can be attributed to the coarse grain composition of these layers, facilitating the movement of microspheres through the voids between the coarse grains, eventually leading to their migration to the collected filtrate samples.

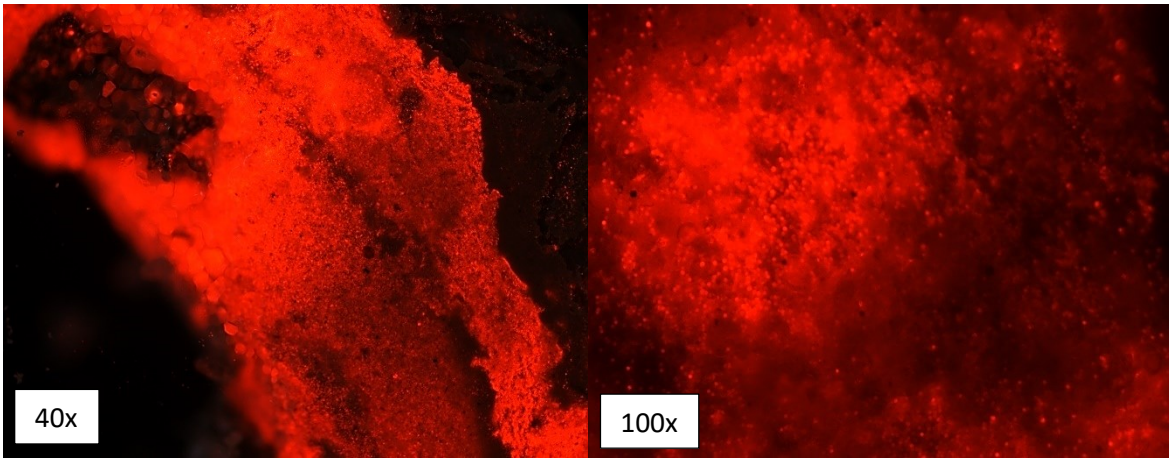

Figure 4-19 Filter cake (upper layer-soil mixture 2, 200 g)

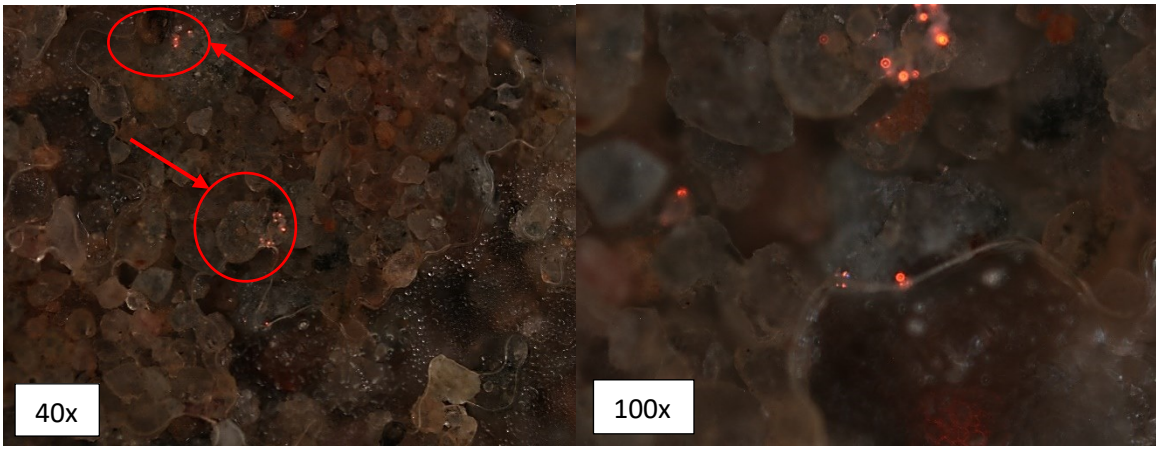

Figure 4-20 Filter cake (middle layer-soil mixture 2, 200 g)

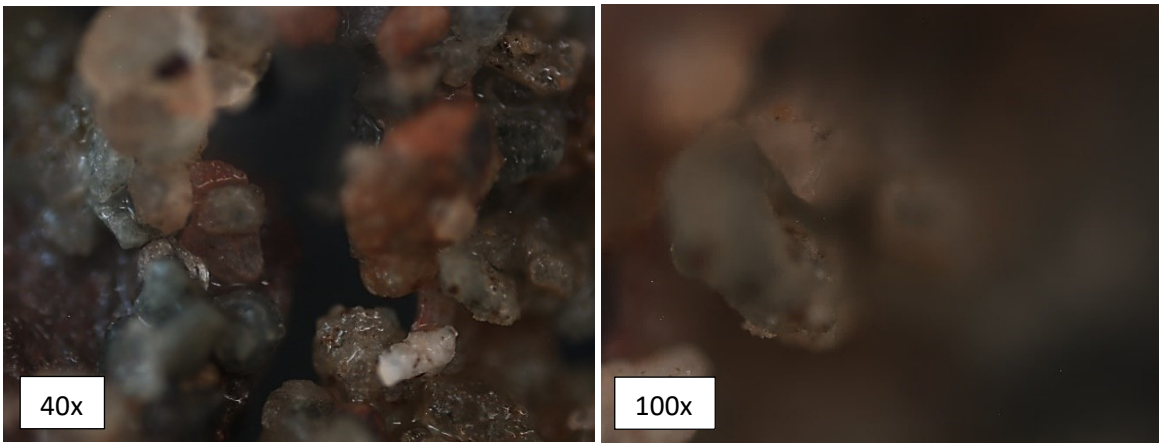

Figure 4-21 Filter cake (bottom layer- soil mixture 2, 200 g)

5 Summary, Conclusions, and Recommendations

5.1 Summary and Conclusions

This chapter provides a summary of the research conducted to develop testing methods to better evaluate particle migration through a geotextile filter cake during dewatering. The chapter also offers a discussion of the main findings and their significance within the context of the research questions, as well as recommendations for future research.

As outlined in the beginning of this thesis, the primary research questions that guided this study were formulated as follows:

- How can we measure microsphere fate and transport in the laboratory during geotextile dewatering?

- What can we use as an experimental test setup to assess the fate and transport of microspheres during the geotextile dewatering process?

An experimental setup was defined to conduct the tests and develop the test method, which involved a layer of geotextile embedded at the bottom of a cylinder for dewatering tests. Experimental methods were developed and adopted using a microscope and fluorescent microspheres. These microsphere visualization and quantification methods were initially assessed through a trial-and-error approach with previous literature forming the basis for the methods.

After development of these methods, experiments with three “steps” (filter cake development, microsphere dewatering, and water filtration) were conducted with different amounts and types of soil to assess microsphere transport. Based on the experimental results and analysis presented in this thesis, the following key findings were identified:

- The test methods developed for microspheres allowed observance of the microsphere movement through various soil filter cakes, both during their initial addition to the filter cake (step 2) and their attempted removal (step 3) with water filtration.
- Quantification methods at various points in each test allowed tracking of microspheres during the test and open up potential avenues for assessing particle migration during dewatering.
- Although not fully developed as a test method, the potential for post-test inspection of filter cake samples also showed promise for investigating particle migration during dewatering.
- It was shown that the test methods employed in this thesis are repeatable, not only for microsphere quantification but also for the various test steps themselves.

It is hoped that the results of this thesis will provide a starting point for others to use these methods to further the understanding of particle transport during dewatering operations. For contaminants with low thresholds of release to the environment (i.e., dioxins and furans) better understanding and help control these contaminants during dewatering.

5.2 Recommendations

Based on the findings and limitations of this research, several recommendations are made for future research in this area.

1. The effectiveness of different soils in dewatering applications can be explored with some of the methods presented in this thesis. In particular, the use of different

colours of fluospheres to examine attachment and detachment mechanisms could be employed.

2. The use of other advanced measurement tools and techniques, such as flow cytometry may provide additional insights into the fate and transport of particles.
3. The methods employed in this research can be used for other studies related to soil filtration studies such as dams or construction related problems where geotextiles are used.
4. The methods employed in this research can be investigated for other research related to soil erosion and particle tracking in these applications.

References

Alimohammadi, M., Tackley, H., Holmes, B., Davidson, K., Lake, C. B., Spooner, I. S., ... & Walker, T. R. (2020). Characterising sediment physical property variability for bench-scale dewatering purposes. Environmental Geotechnics, 40(XXXX), 1-9.

Alimohammadi, M., Tackley, H. A., Lake, C. B., Spooner, I., Walker, T. R., Jamieson, R., ... & Bossy, K. (2020). Effect of different sediment dewatering techniques on subsequent particle sizes in industrial derived effluent. Canadian Journal of Civil Engineering, 47(10), 1145-1153.

Alimohammadi, M. (2020). Fate and transport of particulate matter in geotextile tube dewatering of dioxin and furans contaminated sediments.

Alimohammadi, M., & Lake, C. (2022). Fate and transport of particle matter during geotextile tube dewatering of a dioxin and furan (PCDD/F) contaminated sediment. Geotextiles and Geomembranes, 50(2), 203-215.

Alimohammadi, M., Tackley, H., Holmes, B., Davidson, K., Lake, C. B., Spooner, I. S., ... & Walker, T. R. (2019, May). Laboratory and field physical property characterization for a contaminated sediment for bench scale dewatering purposes. In Geo-Environmental Engineering Conference.

Becker, M. W., Collins, S. A., Metge, D. W., Harvey, R. W., & Shapiro, A. M. (2004). Effect of cell physicochemical characteristics and motility on bacterial transport in groundwater. Journal of Contaminant Hydrology, 69(3-4), 195-213.

Berilgen, S. A., & Bulut, B. T. (2016). Laboratory investigations for dewatering of golden horn dredged sludge with geotextile tubes. Marine Georesources & Geotechnology, 34(7), 638-647.

Bhatia, S. K., & Liao, K. (2005). Geotextile tube: filtration performance of woven geotextiles under pressure. North American Geosynthetic Conference.

Bhatia, S. K., Maurer, B. W., Khachan, M. M., Grzelak, M. D., & Pullen, T. S. (2013). Performance indices for unidirectional flow conditions considering woven geotextiles and sediment Slurries. Sound Geotechnical Research to Practice: Honoring Robert D. Holtz II, 230, 319-333.

Bradford, S. A., & Torkzaban, S. (2008). Colloid transport and retention in unsaturated porous media: A review of interface-, collector-, and pore-scale processes and models. Vadose Zone Journal, 7(2), 667-681.

Bradford, S. A., Torkzaban, S., Kim, H., & Simunek, J. (2012). Modeling colloid and microorganism transport and release with transients in solution ionic strength. Water Resources Research, 48(9).

Camesano, T. A., Unice, K. M., & Logan, B. E. (1999). Blocking and ripening of colloids in porous media and their implications for bacterial transport. Colloids and Surfaces A: Physicochemical and Engineering Aspects, 160(3), 291-307.

Cey, E. E., Rudolph, D. L., & Passmore, J. (2009). Influence of macroporosity on preferential solute and colloid transport in unsaturated field soils. Journal of Contaminant Hydrology, 107(1-2), 45-57.

Chattopadhyay, S., & Puls, R. W. (2000). Forces dictating colloidal interactions between viruses and soil. Chemosphere, 41(8), 1279-1286.

Chowdhury, I., Mansukhani, N. D., Guiney, L. M., Hersam, M. C., & Bouchard, D. (2015). Aggregation and stability of reduced graphene oxide: complex roles of divalent cations, pH, and natural organic matter. Environmental science & technology, 49(18), 10886-10893.

Chowdhury, I., Mansukhani, N.D., Guiney, L.M., Hersam, M.C., & Bouchard, D. (2015). Aggregation and Stability of Reduced Graphene Oxide: Complex Roles of Divalent Cations, pH, and Natural Organic Matter. Environmental Science & Technology, 49(18), 10886-10893.

Close, M. E., Pang, L., Flintoft, M. J., & Sinton, L. W. (2006). Distance and flow effects on microsphere transport in a large gravel column. Journal of environmental quality, 35(4), 1204-1212.

Corapcioglu, M. Y., & Jiang, S. (1993). Colloid-facilitated groundwater contaminant transport. Water Resources Research, 29(7), 2215-2226.

de Jonge, L. W., Kjærgaard, C., & Moldrup, P. (2004). Colloids and colloid-facilitated transport of contaminants in soils: An introduction. Vadose Zone Journal, 3(2), 321-325.

DeNovio, N. M., Saiers, J. E., & Ryan, J. N. (2004). Colloid movement in unsaturated porous media: Recent advances and future directions. Vadose Zone Journal, 3(2), 338-351.

Dong, S., Sun, Y., Gao, B., Shi, X., Xu, H., Wu, J., & Wu, J. (2017). Retention and transport of graphene oxide in water-saturated limestone media. Chemosphere, 180, 506-512.

Espinasse, B., Hotze, E. M., & Wiesner, M. R. (2007). Transport and retention of colloidal aggregates of C60 in porous media: effects of organic macromolecules, ionic composition, and preparation method. Environmental science & technology, 41(21), 7396-7402.

Fan, W., Jiang, X., Lu, Y., Huo, M., Lin, S., & Geng, Z. (2015). Effects of surfactants on graphene oxide nanoparticles transport in saturated porous media. Journal of Environmental Sciences, 35, 12-19.

Feriancikova, L., & Xu, S. (2012). Deposition and remobilization of graphene oxide within saturated sand packs. Journal of hazardous materials, 235, 194-200.

Flury, M., & Qiu, H. (2008). Modeling colloid-facilitated contaminant transport in the vadose zone. Vadose Zone Journal, 7(2), 682-697.

Fowler, J., Bagby, R. M., & Trainer, E. (1996, September). Dewatering sewage sludge with geotextile tubes. In Proceedings of the 49th Canadian Geotechnical Conference (pp. 1-31). Canadian Geotechnical Society, St. John's, NL, Canada.

Gannon, J. T., Manilal, V. B., & Alexander, M. (1991). Relationship between cell surface properties and transport of bacteria through soil. Applied and environmental microbiology, 57(1), 190-193.

Godinez, I. G., & Darnault, C. J. (2011). Aggregation and transport of nano-TiO2 in saturated porous media: effects of pH, surfactants and flow velocity. Water research, 45(2), 839-851.

Grolimund, D., Elimelech, M., Borkovec, M., Barmettler, K., Kretzschmar, R., & Sticher, H. (1998). Transport of in situ mobilized colloidal particles in packed soil columns. Environmental Science & Technology, 32(22), 3562-3569.

Dunphy Guzman, K. A., Finnegan, M. P., & Banfield, J. F. (2006). Influence of surface potential on aggregation and transport of titania nanoparticles. Environmental science & technology, 40(24), 7688-7693.

Harvey, R. W., Kinner, N. E., MacDonald, D., Metge, D. W., & Bunn, A. (1993). Role of physical heterogeneity in the interpretation of small-scale laboratory and field observations of bacteria, microbial-sized microsphere, and bromide transport through aquifer sediments. Water Resources Research, 29(8), 2713-2721.

Huang, C. C., & Luo, S. Y. (2007). Dewatering of reservoir sediment slurry using woven geotextiles. Part I: Experimental results. Geosynthetics International, 14(5), 253-263.

Huang, W., & Koerner, R. M. (2005). An amendment strategy for enhancing the performance of geotextile tubes used in decontamination of polluted sediments and sludges. In Geosynthetics Research and Development in Progress (pp. 1-6).

Jewett, D. G., Hilbert, T. A., Logan, B. E., Arnold, R. G., & Bales, R. C. (1995). Bacterial transport in laboratory columns and filters: influence of ionic strength and pH on collision efficiency. Water research, 29(7), 1673-1680.

Jin, Y., & Flury, M. (2002). Fate and transport of viruses in porous media. *Advances in agronomy*, *77*, 39-102.

Klauth, P., Bauer, R., Ralfs, C., Ustohal, P., Vanderborght, J., Vereecken, H., & Klumpp, E. (2007). Fluorescence macrophotography as a tool to visualise and quantify spatial distribution of deposited colloid tracers in porous media. Colloids and surfaces A: Physicochemical and engineering aspects, 306(1-3), 118-125.

Koerner, G. R., & Koerner, R. M. (2006). Geotextile tube assessment using a hanging bag test. Geotextiles and Geomembranes, 24(2), 129-137.

Kutay, M. E., & Aydilek, A. H. (2004). Retention performance of geotextile containers confining geomaterials. Geosynthetics International, 11(2), 100-113.

Lahlou, M., Harms, H., Springael, D., & Ortega-Calvo, J. J. (2000). Influence of soil components on the transport of polycyclic aromatic hydrocarbon-degrading bacteria through saturated porous media. Environmental science & technology, 34(17), 3649-3656.

Lawson, C. R. (2008). Geotextile containment for hydraulic and environmental engineering. Geosynthetics International, 15(6), 384-427.

Liao, K. (2008). Dewatering of natural sediments using geotextile tubes. Syracuse University.

Liao, K., & Bhatia, S. K. (2006). Evaluation on Filtration Performance of Woven Geotextiles by Falling Head, Pressure Filtration Test, and Hanging Bag Test.: Eighth International Conference on Geosynthetics.

Lin, S., Cheng, Y., Liu, J., & Wiesner, M. R. (2012). Polymeric coatings on silver nanoparticles hinder autoaggregation but enhance attachment to uncoated surfaces. Langmuir, 28(9), 4178-4186.

Liu, L., Gao, B., Wu, L., Sun, Y., & Zhou, Z. (2015). Effects of surfactant type and concentration on graphene retention and transport in saturated porous media. Chemical Engineering Journal, 262, 1187-1191.

Magal, E., Weisbrod, N., Yechieli, Y., Walker, S. L., & Yakirevich, A. (2011). Colloid transport in porous media: impact of hyper-saline solutions. water research, 45(11), 3521-3532.

Mastin, B. J., Lebster, G. E., & Salley, J. R. (2008). Use of Geotube® dewatering containers in environmental dredging. In GeoAmericas Conference Proceedings (pp. 1467-1486).

McDowell-Boyer, L. M., Hunt, J. R., & Sitar, N. (1986). Particle transport through porous media. Water Resources Research, 22(13), 1901-1921.

Minitab, LLC. (2021). Minitab Statistical Software (Version 21.2) [Computer software]. Minitab, LLC.

Mishurov, M., Yakirevich, A., & Weisbrod, N. (2008). Colloid transport in a heterogeneous partially saturated sand column. Environmental Science & Technology, 42(4), 1066-1071.

Molnar, I. L., Johnson, W. P., Gerhard, J. I., Wilson, C. S., & O'Carroll, D. M. (2015). Predicting colloid transport through saturated porous media: A critical review. Water Resources Research, 51(9), 6804-6845.

Moo-Young, H. K., Gaffney, D. A., & Mo, X. (2002). Testing procedures to assess the viability of dewatering with geotextile tubes. Geotextiles and Geomembranes, 20(5), 289-303.

Moo-Young, H., & Ochola, C. (1999). Laboratory evaluation of geosynthetic fabric containers for contaminant migration. Lehigh Univ., Bethlehem, PA (US).

Mori, H., Miki, H., & Tsuneoka, N. (2002). The geo-tube method for dioxin-contaminated soil. Geotextiles and Geomembranes, 20(5), 281-288.

Muthukumaran, A. E., & Ilamparuthi, K. (2006). Laboratory studies on geotextile filters as used in geotextile tube dewatering. Geotextiles and Geomembranes, 24(4), 210-219.

Ochiai, N., Dragila, M. I., & Parke, J. L. (2010). Three-Dimensional Tracking of Colloids at the Pore Scale Using Epifluorescence Microscopy. Vadose Zone Journal, 9(3), 576-587.

Ouyang, Y., Shinde, D., Mansell, R. S., & Harris, W. (1996). Colloid-enhanced transport of chemicals in subsurface environments: A review. Critical Reviews in Environmental Science and Technology, 26(2), 189-204.

Petosa, A. R., Jaisi, D. P., Quevedo, I. R., Elimelech, M., & Tufenkji, N. (2010). Aggregation and deposition of engineered nanomaterials in aquatic environments: role of physicochemical interactions. Environmental science & technology, 44(17), 6532-6549.

Porubcan, A. A., & Xu, S. (2011). Colloid straining within saturated heterogeneous porous media. Water Research, 45(4), 1796-1806.

Qi, Z., Zhang, L., & Chen, W. (2014). Transport of graphene oxide nanoparticles in saturated sandy soil. Environmental Science: Processes & Impacts, 16(10), 2268-2277.

Grasso, D., Subramaniam, K., Butkus, M., Strevett, K., & Bergendahl, J. (2002). A Review of Non-DLVO Interactions in Environmental Colloidal Systems. Reviews in Environmental Science and Biotechnology, 1(1), 17-38.

Razali, N. M., & Wah, Y. B. (2011). Power comparisons of shapiro-wilk, kolmogorov-smirnov, lilliefors and anderson-darling tests. Journal of statistical modeling and analytics, 2(1), 21-33.

Ryan, J. N., & Elimelech, M. (1996). Colloid mobilization and transport in groundwater. Colloids and surfaces A: Physicochemical and engineering aspects, 107, 1-56.

Ryan, J. N., & Gschwend, P. M. (1994). Effects of ionic strength and flow rate on colloid release: Relating kinetics to intersurface potential energy. Journal of colloid and interface science, 164(1), 21-34.

Satyamurthy, R. (2008). Experimental investigations of geotextile tube dewatering.

Segre, G. (2013). A physicochemical evaluation of the compressibility and dewatering behavior of dredged sediments (Doctoral dissertation, Syracuse University).

Sen, T. K., & Khilar, K. C. (2006). Review on subsurface colloids and colloid-associated contaminant transport in saturated porous media. Advances in colloid and interface science, 119(2-3), 71-96.

Sharma, P. K., & McInerney, M. J. (1994). Effect of grain size on bacterial penetration, reproduction, and metabolic activity in porous glass bead chambers. Applied and Environmental Microbiology, 60(5), 1481-1486.

Shirvan, A. R., Nouri, A., & Wen, C. (2021). Structural polymer biomaterials. In Structural Biomaterials (pp. 395-439). Woodhead Publishing.

Sobsey, M. D., & Meschke, J. S. (2003). Virus survival in the environment with special attention to survival in sewage droplets and other environmental media of fecal or respiratory origin. Report for the World Health Organization, Geneva, Switzerland, 70.

Stumm, W. (1977). Chemical interaction in particle separation. Environmental Science & Technology, 11(12), 1066-1070.

Sun, Y., Gao, B., Bradford, S. A., Wu, L., Chen, H., Shi, X., & Wu, J. (2015). Transport, retention, and size perturbation of graphene oxide in saturated porous media: effects of input concentration and grain size. Water research, 68, 24-33.

Tackley, H. (2019). The Behavior and Migratory Fate of Select Heavy Metals During the Dewaterment of an Effluent Derived Sediment.

Tackley, H. A., Lake, C. B., & Alimohammadi, M. (2021). Examining metal migration through geotextiles during dewatering. Geotextiles and Geomembranes, 49(1), 32-40.

TenCate Corporation. (2015). Geotube® Dewatering Container (Standard Dewatering Specification). Version 15.

Thio, B. J. R., Montes, M. O., Mahmoud, M. A., Lee, D. W., Zhou, D., & Keller, A. A. (2012). Mobility of capped silver nanoparticles under environmentally relevant conditions. Environmental science & technology, 46(13), 6985-6991.

Tian, Y. A., Gao, B., Silvera-Batista, C., & Ziegler, K. J. (2010). Transport of engineered nZnO in saturated porous media. Journal of Nanoparticle Research, 12(7), 2371–2380.

Tong, M., Li, X., Brow, C. N., & Johnson, W. P. (2005). Detachment-influenced transport of an adhesion-deficient bacterial strain within water-reactive porous media. Environmental Science & Technology, 39(8), 2500-2508.

Vecchia, E. D., Luna, M., & Sethi, R. (2009). Transport in porous media of highly concentrated iron micro- and nanoparticles in the presence of xanthan gum. Environmental Science & Technology, 43(23), 8942-8947.

Wang, M., Gao, B., Tang, D., Sun, H., Yin, X., & Yu, C. (2017). Effects of temperature on graphene oxide deposition and transport in saturated porous media. Journal of hazardous materials, 331, 28-35.

Wang, Y., Li, Y., Costanza, J., Abriola, L. M., & Pennell, K. D. (2012). Enhanced mobility of fullerene (C60) nanoparticles in the presence of stabilizing agents. Environmental science & technology, 46(21), 11761-11769.

Weggel, J. R., & Ward, N. D. (2012). A model for filter cake formation on geotextiles: Theory. Geotextiles and Geomembranes, 31, 51-61.

Williamson, D., Lynch-Wood, G., & Ramsay, J. (2006). Drivers of environmental behaviour in manufacturing SMEs and the implications for CSR. Journal of business ethics, 67, 317-330.

Yee, T. W., & Lawson, C. R. (2012). Modelling the geotextile tube dewatering process. Geosynthetics International, 19(5), 339-353.

Yee, T. W., Lawson, C. R., Wang, Z. Y., Ding, L., & Liu, Y. (2012). Geotextile tube dewatering of contaminated sediments, Tianjin Eco-City, China. Geotextiles and Geomembranes, 31, 39-50.

Zhang, J., Guo, W., Li, Q., Wang, Z., & Liu, S. (2018). The effects and the potential mechanism of environmental transformation of metal nanoparticles on their toxicity in organisms. Environmental Science: Nano, 5(11), 2482-2499.

Zvikelsky, O., & Weisbrod, N. (2006). Impact of particle size on colloid transport in discrete fractures. Water Resources Research, 42(12).

Zvikelsky, O., Weisbrod, N., & Dody, A. (2008). A comparison of clay colloid and artificial microsphere transport in natural discrete fractures. Journal of Colloid and Interface Science, 323(2), 286-292.